Diploma thesis

Effects of Novel Anticancer Therapies on Cardiac Calcium Homeostasis

submitted by

Christopher Schneider

for the academic degree of

Doctor medicinae universae

(Dr. med. univ.)

at the

Medical University of Graz

conducted at the

Division of Cardiology
Department of Internal Medicine

under supervision of

Ass.-Prof. Priv.-Doz. Dr.med. Dr.scient.med. Peter Rainer
Ass.-Prof. Priv.-Doz. Dr.rer.nat. Simon Sedej

Graz, 15 March 2017

Statutory declaration

I declare on honour that I have authored this thesis independently, that I have not used other than the declared sources / resources, and that I have explicitly marked all material which has been quoted either literally or by content from the used sources.

Graz, 15 March 2017 *Christopher Schneider eh.*

Preface

I have always been interested in two things: physics and medicine. The logic behind both fascinated me. How is the world constructed, how does the body – my body – work? So, after finishing a college of electronics specialising in telecommunication I had to decide which of those paths to choose. After careful consideration of my options and a year working as a paramedic at the Red Cross, I finally decided to pursue a career in medicine. It was compelling for me to combine the logic of physiology and pathology and apply it in real life to help people. It may sound rather naïve, but despite of hearing about long night shifts and a lot of paperwork, I could not withstand the urge to follow my passion.

After managing the entrance exam, time flew by very quickly. But a new problem emerged soon after. Which field should I later specialise in? Over the course of time and after spending even more time as a paramedic at night shifts and after a great deal of clinical traineeships it became clear that emergency medicine, anaesthesiology, and cardiology are my main fields of interest. Especially understanding the heart itself was crucial in all three fields. So, when I found out about Dirk von Lewinski offering a research topic for a thesis in cardiology I called him immediately, but due to the late starting point I had to decline his offer. Luckily, he brought me into contact with Peter Rainer, who gave me the chance to start instantly and still work in basic research. Studying the effects of novel anticancer therapies on the heart turned out to be a really fascinating but time-consuming topic. It took me a lot of effort to finally get viable cells and results. After almost one and a half years of ongoing experiments, programming, and writing it finally paid off. The following pages are the compressed form of this hard work. But do not get me wrong, I absolutely do not want to miss these times. I have learned a lot, I think more rationally now and am able to scrutinise even big and complex papers. I met a lot of new people and visited interesting congresses where I presented some of my preliminary data. These experiences are indispensable for my future career, whether it will be in research, clinics, or both.

I hope that with this thesis I contribute to a better understanding of the working heart and the influence of drugs on it, and to a better quality of life of patients who already have to suffer from cancer itself. The treatment should not make their lives even more difficult.

Acknowledgements

I want to express my sincere gratitude to my supervisor Peter Rainer, who has given me the opportunity to become part of the scientific community enabling me to pursuit my interests in basic science in the field of cardiology. His knowledge, unwavering enthusiasm, and keen interest in this topic encouraged me to submerge myself in this topic. Without his constant support, critical advices, and continuous supervision this thesis would not have been possible.

I would also like to thank my co-supervisor Simon Sedej for his patience in showing me the required methods for my thesis and his expertise and critical suggestions. Even in times of trouble, when I could not find any solution, he always had an idea in the back of his head to improve my protocol.

For providing the starting point of my thesis, I want to thank Markus Wallner, Dirk von Lewinski, Martin Pichler, and again Peter Rainer. Without their muscle strip experiments, I would have lacked the fundamental basis for my subsequent work.

I also want to thank Eva Thon-Gutschi and Viktoria Herbst for keeping the lab running and always giving me a helping hand when I needed one. Especially Eva, who taught me all the molecular biology techniques needed for successfully finishing my thesis.

To my colleagues who eventually became friends, who worked with me late into the nights. A sorrow shared is a sorrow halved. You made it a lot easier. Thank you.

Special thanks goes to my family and friends. Words cannot express how grateful I am for their support in these times. To my brother, my proofreader and best friend, and especially to my parents, I want to express my sincere eternal gratefulness. Although it was not always easy for them, they tirelessly supported me no matter what. Thank you!

Abstract

Background: Tyrosine-kinase inhibitors (TKIs) are widely used in cancer treatment. Despite being more targeted than conventional chemotherapy, TKIs may exhibit substantial cardiotoxicity. Here, we aim to characterise underlying alterations of cardiomyocyte calcium homeostasis caused by the TKI sorafenib in order to identify potential protective co-treatments.

Methods: Intracellular calcium transients (CaTs) were assessed at room temperature using laser scanning microscopy in electrically stimulated (0.5Hz), isolated murine C57BL/6 cardiomyocytes loaded with the calcium-sensitive fluorescent dye Fluo-4/AM (1.5µM). Myocytes were superfused with sorafenib (10µM) or vehicle control (n=21 and 20 cells, respectively, 7 hearts). Isoproterenol- (10nM) and caffeine-induced (30mM) responses were measured to assess beta-adrenergic reserve and sarcoplasmic reticulum (SR) calcium content, respectively. Western blots were performed for calcium-handling proteins phospholamban (PLB) and Ca^{2+}/calmodulin-dependent protein kinase II (CaMKII), including their phosphorylated forms pPLB S16, pPLB T17, and pCaMKII T286. Custom-made R scripts were used for CaTs and Western blot analyses, and statistical testing.

Results: Sorafenib-superfused cardiomyocytes showed a progressive decrease in systolic calcium transient amplitude reaching 52±8.1% of the baseline amplitude at the maximum drug effect ($p<0.001$), while control cells did not show any significant difference in CaT peak amplitude over time ($p=0.93$). Calcium release and re-uptake kinetics were negatively altered ($p<0.05$) by sorafenib resulting in slower increase and decrease of CaTs, respectively. Beta-adrenergic stimulation with isoproterenol increased transient amplitude in control myocytes, which was attenuated in sorafenib-treated cells ($p<0.001$). Furthermore, sorafenib significantly reduced SR calcium content compared to control ($p<0.05$), with a trend toward prolonged decay time (Tau constant) of the caffeine-induced response ($p=0.063$). Western blots showed reduced phosphorylation of PLB at serine 16 and a trend towards reduced phosphorylation at threonine 17. CaMKII phosphorylation was not significantly altered.

Summary: Immediate negative inotropy by sorafenib is associated with reduced SR Ca^{2+} load, likely due to impaired SERCA2a function caused by reduced PLB phosphorylation at serine 16 leading to a decrease of intracellular CaT peak amplitude. Furthermore, SR calcium release and re-uptake parameters are altered by sorafenib: SR calcium content is decreased and calcium release and re-uptake kinetics are slowed.

Zusammenfassung

Hintergrund: Tyrosinkinase-Inhibitoren (TKIs) finden in der Krebsbehandlung weite Verbreitung. Obwohl zielgerichteter als herkömmliche Chemotherapeutika, scheint ihr Kardiotoxizitätsrisiko erheblich höher zu sein als angenommen. Mit der vorliegenden Studie versuchen wir die zugrundeliegenden Veränderungen der Kalziumhomöostase von Kardiomyozyten durch den TKI Sorafenib zu charakterisieren um potentiell protektive adjuvante Behandlungen identifizieren zu können.

Methoden: Intrazelluläre Kalziumtransienten (CaTs) von isolierten murinen C57BL/6-Kardiomyozyten, beladen mit dem kalziumsensitiven Fluoreszenzfarbstoff Fluo-4/AM (1.5µM), wurden bei Raumtemperatur mit einem Laserscanningmikroskop unter elektrischer Stimulation (0.5Hz) gemessen. Myozyten wurden mit Sorafenib (10µM) oder mit dem Trägerstoff (Kontrolle) superfundiert (n=21 beziehungsweise 20 Zellen, 7 Herzen). Isoproterenol- (10nM) und koffeininduzierte (30mM) Transienten wurden gemessen, um die beta-adrenerge Reserve respektive den Kalziumgehalt des sarkoplasmatischen Retikulums zu bestimmen. Western blots wurden für die an der Kalziumhomöostase beteiligten Proteine Phospholamban (PLB) und Ca^{2+}/Calmodulin-abhängige Proteinkinase II (CaMKII) und deren phosphorylierte Formen pPLB S16, pPLB T17 und pCaMKII T286 durchgeführt. Individuelle R-Scripts wurden für die CaTs- und Western-Blot-Analysen und für die statistischen erstellt.

Ergebnisse: Sorafenib-superfundierte Kardiomyozyten zeigten eine progrediente Abnahme der systolischen Kalziumtransientenamplituden von 52±8,1% der Ausgangsamplituden zum Zeitpunkt des maximalen pharmakologischen Effektes ($p<0,001$), während die Kontrollzellen über die Zeit überhaupt keinen signifikanten Unterschied der CaT-Amplituden aufwiesen ($p=0,93$). Kalziumfreisetzung und –wiederaufnahme wurden durch Sorafenib negativ beeinflusst ($p<0,05$). Dies führte zu einem langsameren Anstieg und Abfall der CaTs. Beta-adrenerge Stimulation mit Isoproterenol erhöhte die Transientenamplituden in den Kontrollzellen, während diese Antwort in den mit Sorafenib behandelten Zellen abgeschwächt war ($p<0,001$). Weiters führte Sorafenib, verglichen mit der Kontrollgruppe, zu einer signifikanten Reduktion des SR-Kalziumgehalts ($p<0,05$) mit dem Trend zu einer verlängerten Abfallzeit (Tau) der koffeininduzierten Antwort ($p=0,063$). Western blots zeigten eine reduzierte Phosphorylierung von PLB an Serin 16 und einen Trend zu einer reduzierten

Phosphorylierung an Threonin 17. CaMKII-Phosphorylierung wurde nicht signifikant beeinflusst.

Diskussion: Umgehende negative inotrope Effekte durch Sorafenib, die zu einer Reduktion der intrazellulären Spitzenamplitude der CaTs führen, sind assoziiert mit einem reduzierten SR-Ca^{2+}-Gehalt, wahrscheinlich verursacht durch beeinträchtigte SERCA2a-Funktion aufgrund von PLB-Phosphorylierung an Serine 16. Weiters werden Kalziumfreisetzung und –wiederaufnahme des SRs verändert: Der SR-Kalziumgehalt ist reduziert und die Kalziumfreisetzung und –wiederaufnahmeparameter sind verlangsamt.

Table of Contents

Glossary and Abbreviations

A

Abl	Abelson murine leukemia viral oncogene homologue
Ack	activated CDC42 kinase
ANOVA	analysis of variance
approx.	approximately
ATP	adenosine triphosphate

B

BCA	bichinchoninic acid
BSA	bovine serum albumin

C

CaMKII	Ca^{2+}/calmodulin-dependent protein kinase II
c-kit	mast/stem cell growth factor receptor
CLB	cell lysis buffer
CML	chronic myelogenous leukemia
Csk	C-terminal Src (sarcoma) kinase

D

ddH_2O	double-distilled water
DMSO	dimethyl sulfoxide

E

ECC	excitation-contraction coupling
EF	ejection fraction
EGFR	epidermal growth factor receptor
ErbB2	=HER2/neu (human epidermal growth factor receptor 2)
ERK	extracellular signal-regulated kinase

F

Fac	focal adhesion kinase
Fes/Fer kinases	feline sarcoma/Fes-related kinases
FDA	U.S. Food and Drug Administration
Flt-3	fms(Feline McDonough Sarcoma)-like tyrosine kinase 3
FS	fractional shortening

G

GAPDH	glyceraldehyde 3-phosphate dehydrogenase
GIST	gastrointestinal stromal tumour

H

hiPSC-CM	human induced pluripotent stem cell derived cardiomyocytes

I

IGFR	insulin-like growth factor receptor

i.p.	intraperitoneal
I.U.	international unit
J	
Jak	Janus kinase
L	
LD_{50}	median lethal dose
LTCC	L-type calcium channel
M	
MedDRA	Medical Dictionary for Regulatory Activities
MEK	mitogen-activated protein kinase kinase
min	minute
MKI	multi-target tyrosine-kinase inhibitor
N	
NCX	sodium-calcium exchanger
NRTK	non-receptor tyrosine kinase
NT	normal Tyrode
NT-proBNP	N-terminal pro b-type natriuretic peptide
P	
p38α	p38 mitogen-activated protein kinases α
PDGFR	platelet-derived growth factor receptors
Ph+ ALL	Philadelphia chromosome positive acute lymphoblastic leukaemia
PKA	protein kinase A
PLB	phospholamban
PMCA	Plasma membrane Ca^{2+} ATPase
PMSF	phenylmethylsulfonyl fluoride
PTM	post-translational modification
R	
rpm	revolutions per minute
Raf kinase	rapidly accelerated fibrosarcoma kinase
RT	room temperature
RT10	relaxation time 10% of maximum
RT50	relaxation time 50% of maximum
RTK	receptor tyrosine kinase
RyR	ryanodine receptor
S	
Ser16	serine at position 16
SERCA	sarcoendoplasmic reticulum Ca^{2+} ATPase (in cardiomyocytes primarily as isoform SERCA2a)
SR	sarcoplasmic reticulum
Src	sarcoma kinase
stim.	stimulated

Syk/Zap70	spleen tyrosine kinase/zeta-chain-associated protein kinase 70
T	
TACE	transcatheter arterial chemoembolisation
tau	relaxation time 1/e of maximum
Tec	family of five kinases (Tec, Btk, Itk/Emt/Tsk, Rlk/Txk, Bmx/Etk)
Thr17	threonine at position 17
TK	tyrosine kinase
TKI	tyrosine-kinase inhibitor
TRPC channel	transient receptor potential cation channel
V	
VEGFR	vascular endothelial growth factor receptor
W	
WB	Western blot

List of figures

List of tables

1 Introduction

1.1 Overview

Before the discovery of Tyrosine-kinase inhibitors (TKIs) in 1988 (1), the cornerstone of cancer treatment was targeting cell proliferation with cytotoxic agents. This often resulted in significant side effects on other rapidly dividing cells like bone marrow, hair follicles, and cells in the gastrointestinal and reproductive systems. Therefore, researchers sought to better define molecular targets and specifically impact these with fewer side effects. The first TKI that was approved was imatinib for the treatment of chronic myeloid leukemia (CML). Since then, the number of TKIs has been growing steadily and enabled more targeted cancer therapies and reduction of potentially fatal side effects. Yet, despite being more targeted, TKIs still exhibit substantial cardiotoxicity (2–5). Here, we aimed to characterise underlying alterations of cardiomyocyte calcium homeostasis in order to identify potential protective co-treatments.

1.2 Tyrosine Kinases

Tyrosine kinases (TKs) are a subgroup of protein kinases catalysing the phosphorylation of the amino acid tyrosine by transferring a phosphate group originating from adenosine triphosphate (ATP). Thereby TKs regulate protein function and cellular signal transduction via post-translational modification of target proteins (6) (**Fig. 1**). TKs play an essential role in cardiac development, physiology and pathology. As key regulators, they are vital for a vast amount of cellular processes, and dysregulations cause severe complications. For example, ErbB2 and 4 blockade leads to dilated cardiomyopathy, whereas a dysfunction of the insulin receptor (IGFR) causes impaired left ventricular contractility (7). TKs can be divided into two main

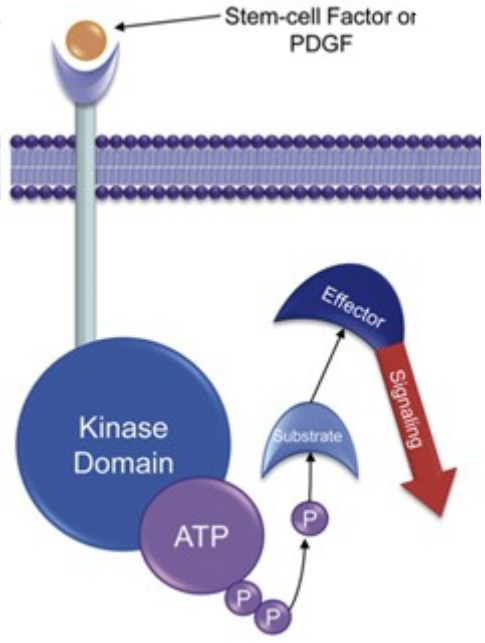

Figure 1 Schematic of mechanism of action of a TK (here PDGF). Adapted from A decade of tyrosine kinase inhibitor therapy, J. Blay (75)

groups, namely receptor tyrosine kinases (RTKs) and non-receptor tyrosine kinases (NRTKs). In contrast to RTKs which have a transmembrane domain, NRTKs, as cytoplasmic enzymes, do not (8).

1.2.1 Receptor tyrosine kinases

RTKs are further divided into 20 subgroups, such as the vascular endothelial growth factor receptor (VEGFR), the platelet-derived growth factor receptor (PDGFR), and the epidermal growth factor receptor (EGFR). They catalyse, as mentioned before, the phosphorylation of the target molecule tyrosine by using ATP as a high-energy donor. As such RTKs regulate key processes that are vital for cancer progression in many cells (8,9), such as cell growth, apoptosis, or neoangiogenesis.

1.2.2 Non-receptor tyrosine kinases

So far, nine families of NRTKs have been described. Although most of them are cytoplasmic, some are bound to the inner layer of the cellular membrane (10). Similar to RTKs, they also use ATP to phosphorylate tyrosine of a protein (8) and are distributed throughout the body. NRTK can be divided into 9 families: Abl, Fes/Fer, Syk/Zap70, Jak, Tec, Fak, Ack, Src, and Csk (8). For example, Janus kinases are playing a critical role in the immune system (11). Abl and Src are both involved in cancer development (12).

1.3 Tyrosine-Kinase Inhibitors

Clinically used TKIs are either monoclonal antibodies or soluble decoy molecules, which bind to a receptor or the ligand. Small-molecule inhibitors represent an additional type of inhibitors blocking ATP or another substrate from attaching to the kinase (13).
By virtue of the great opportunity of targeting cancer by inhibiting the previously mentioned pathways, a substantial number of TKIs have been developed so far. Starting with an EGF-receptor inhibitor in 1988 (1), the first FDA (Food and Drug Administration) -approved TKI was imatinib, used to treat chronic myelogenous leukaemia (CML) by inhibiting Bcr-Abl tyrosine kinase [later research showed further mechanisms of action via c-kit and PDGFR and imatinib was also used for Philadelphia chromosome positive acute

lymphatic leukemia (Ph+ ALL) and gastrointestinal stromal tumours (GIST)]. Imatinib revolutionised the treatment of CML. Later, due to development of imatinib-resistant Bcr-Abl mutants, second generation inhibitors like desatinib or bosutinib have been developed (14,15). Other than leukaemias, TKIs like gefitinib were used to target cancer with overexpressed EGFR such as certain types of lung, breast, or other cancers.

Due to the flexibility of cancer cells with their inherent capability to develop resistances and adapt to therapies (16), targeting multiple oncoproteins instead of one target may be advantageous and multiple single-target TKIs and single multi-target TKIs (MKIs) were developed and used thereafter (17).

1.3.1 Multi-target tyrosine-kinase inhibitors

MKIs are targeting several pathways to improve response rates. First-generation MKIs such as sunitinib, which is used in the treatment of advanced renal cell carcinoma, or imatinib, used as a first-line therapy in CML (18) and further used in resistant/intolerant GIST, as well as sorafenib (details below) are a cornerstone in specific cancer treatments. Most of the second-generation MKIs are currently assessed in clinical trials or have already been approved by either the Food and Drug Administration (FDA) or the European Medicines Agency (EMA) or both (e.g., axitinib, pazopanib). (8)

Second-generation MKIs were developed to increase efficiency while reducing adverse effects and giving an alternative to first-generation MKI-resistant cancer types (19,20).

Nevertheless, TKIs still exhibit substantial side effects and MKIs are by definition not selective and thus have a higher probability of causing toxicity. (17)

1.3.2 Side effects of TKIs

> *"There is increasing evidence that patients whose disease is controlled by TKI's will have greater impact on their quality of life from comorbidities or drug adverse events than from the disease itself."* (21)

Although TKIs have a much better toxicity profile than chemotherapy, side effects are still a major concern using this treatment (for side effects of the TKI sorafenib see **Table 1**). Due to the high expression of RTKs in the human body, adverse reactions reach from the

cardiovascular system, sensory system, metabolism, skin, liver, to the haematological system (5,15).

Table 1 All adverse sorafenib reactions reported in patients in multiple clinical trials in Medical Dictionary for Regulatory Activities (MedDRA) Coding (22)

System / Organ / Class Disorders	**Very Common ≥10%**	**Common ≥1% to <10%**	**Uncommon ≥0.1% to <1%**	**Rare ≥0.01% to <0.1%**
Infections and Infestation	infection	folliculitis		
Blood and Lymphatic System	lymphopenia	leucopoenia neutropenia anaemia thrombocytopenia		
Immune System			anaphylactic reaction hypersensitivity reactions (including skin reactions and urticaria)	
Endocrine		hypothyroidism	hyperthyroidism	
Metabolism and Nutrition	anorexia hypophosphataemia	hypocalcaemia hypokalemia hyponatraemia	dehydration	
Psychiatric		depression		
Nervous System		peripheral sensory neuropathy dysgeusia	reversible posterior leukoencephalopathy*	
Ear and Labyrinth		tinnitus		
Cardiac		congestive heart failure* myocardial ischaemia and/or infarction*		QT prolongation
Vascular	haemorrhage (inc. gastrointestinal*, respiratory tract* and cerebral haemorrhage*) hypertension	flushing	hypertensive crisis*	
Respiratory, Thoracic and Mediastinal		rhinorrhoea dysphonia	interstitial lung disease-like events* (includes reports of pneumonitis, radiation pneumonitis, acute respiratory distress, interstitial pneumonia, pulmonitis and lung inflammation)	
Gastrointestinal	diarrhoea nausea vomiting constipation	stomatitis (including dry mouth and glossodynia)	pancreatitis gastritis gastrointestinal perforations*	

		dyspepsia dysphagia gastrooesophageal reflux disease		
Hepato-biliary			increase in bilirubin and jaundice, cholecystitis, cholangitis	drug-induced hepatitis*
Skin and Subcutaneus Tissue	dry skin rash alopecia hand foot skin reaction** erythema pruritus	keratoacanthoma/ squamous cell cancer of skin dermatitis exfoliative acne skin desquamation hyperkeratosis	eczema erythema multiforme drug	
Musculoskeletal, Connective Tissue and Bone	arthralgia	myalgia muscle spasms		
Renal and Genitourinary		renal failure proteinuria		nephrotic syndrome
Reproductive System and Breast		erectile dysfunction	gynaecomastia	
General Disorders and Administration Site Conditions	fatigue pain (including mouth, abdominal, bone, tumour pain and headache) fever	asthenia influenza like illness mucosal inflammation		
Investigations	weight decreased increased amylase increased lipase	transient increase in transaminases	transient increase in blood alkaline phosphatase INR abnormal, prothrombin level abnormal	

* The adverse reactions may have a life-threatening or fatal outcome.

** palmar plantar erythrodysaesthesia syndrome in MedDRA

1.3.2.1 Cardiotoxic side effects of conventional chemotherapies

Before describing the cardiotoxicity of TKIs in detail, it is necessary to set them into perspective to conventional chemotherapies. Some of the most common classical chemotherapeutic agents in use are anthracyclines. They exhibit substantial dose-dependent cardiotoxicity in up to 5% of treated patients leading to an irreversible non-ischemic toxic cardiomyopathy. Another group are fluorpyrimidines causing cardiac events in 7.6% probably due to endothelial dysfunction and vasospasms of coronary arteries, but the exact origin of cardiotoxicity is still unknown. (23)

Taxanes and cyclophosphamides, two further conventional chemotherapeutic agents, do not cause or lack severe cardiotoxicity (left ventricular dysfunction, ischemia) in most cases. Nonetheless, taxanes lead to subclinical sinus bradycardia in approx. 30% of treated

patients and cyclophosphamides may induce acute pericarditis if administered at high dose (23).

1.3.2.2 Cardiotoxic side effects of TKIs

Causes of dose-dependent, and often irreversible cardiotoxic effects of conventional chemotherapeutics are generally well understood and predictable. This stands in contrast to TKIs, as our understanding of those is still limited.

Developed to enhance the efficacy while reducing the side effects, cardiotoxic manifestations such as heart failure or myocardial ischemia, are still one of the major limitations in cancer treatment with TKIs due to significant repercussions on patient outcomes (23,24). In 2013, a study performed on 159 advanced renal cell carcinoma patients treated with a TKI, showed that 33% developed some kind of cardiovascular toxicity {using Common Terminology Criteria for Adverse Events version 4.0; heart failure ≥°I [asymptomatic with laboratory [NT-proBNP levels (>300 pg/ml) or an increase by at least 100% of a previously elevated level] or cardiac imaging abnormalities], ejection fraction (EF) decrease ≥°II (resting EF 50%-40%; 10%-19% drop from baseline), elevated Troponin I ≥°I (levels above the upper limit of normal and below the level of myocardial infarction) and hypertension ≥°2 (stage 1 hypertension)} (25). In a study conducted in 2008, in 18% of patients treated with sorafenib or sunitinib, symptomatic cardiac side effects (angina, dyspnea, and dizziness) occurred (3). But regarding serious ischaemic heart events with hospitalisation, Srikanthan et al. showed 2015 similar outcomes compared to age- and gender-matched non-cancer patients (26).

Compared to classical chemotherapy, little is known about the mechanisms underlying these cardiotoxicities in emerging cancer therapeutics, especially in TKIs (2). On-target effects are easier to understand since some targeted kinases also play an important role in the heart. Off-target effects are primarily caused by a lack of absolute selectivity. For example, sunitinib was originally developed to inhibit VEGFR, PDGFR, and c-kit but turned out to inhibit over 50 kinases (27). Therefore, it is difficult or even impossible to attribute cardiotoxicity to certain TKs. But the inhibition of VEGF for example has been identified to lead to endothelial dysfunction and may cause hypertension, thrombosis, or bleeding. Furthermore, VEGF levels are increased in pre-damaged hearts leading to the hypothesis that the inhibition of this signal pathway deteriorates existing conditions (28).

At present, the acute effects of TKI on cardiac contractility in human samples and underlying calcium changes and post-translational modifications (PTMs) remain ill-defined. Here, we aim to close this knowledge gap.

Before hypothesising about possible mechanisms, background information on cardiac contraction and cardiomyocyte calcium cycling is needed.

Excitation-contraction coupling (ECC) is the conversion of an incoming electrical stimulus to a mechanical response. In the heart, the sinoatrial node sets the pace by spontaneously generating an action potential which eventually reaches the myocytes and ultimately causes them to contract. This is caused by a chain reaction in the cell starting with a rapid Na^+ influx due to increased conductivity. In phase 2 of the action potential Ca^{2+} enters the cell through L-type calcium channels leading to a subsequent Ca^{2+} release from sarcoplasmic reticulum (SR) via ryanodine receptors (RyR) (calcium-induced calcium release) increasing cytosolic Ca^{2+} from ≈100 nmol/L to ≈1 µmol/L (29). The high concentration allows Ca^{2+} to bind to the myofilament protein troponin C enabling a troponin I conformation change exposing actin to bind to myosin ATPase on the myosin head. ATP hydrolysis then provides energy for a conformational change of the actin-myosin complex driving the movement between actin and the head of myosin. Not before calcium concentration decreases, troponin I inhibits actin-myosin binding and ATP binds to the myosin head, re-establishing initial length. Responsible for calcium decrease is the slowing of influx and the active removal through SERCA (sarcoendoplasmic reticulum Ca^{2+} ATPase) and NCX (sodium-calcium exchanger). While SERCA is essential for calcium removal and cell relaxation, it is also crucial for the following contraction as it pumps calcium back into the SR (sarcoplasmic reticulum). The higher the concentration of calcium in the SR, the stronger the next potential contraction. (30–32)

In this chain of reactions, we wanted to find potential causative factors for negative inotropy, which may include dephosphorylated phospholamban (PLB), a regulator inhibiting calcium uptake into the SR if not phosphorylated, dephosphorylated L-type calcium channel (LTCC), de-sensitised troponin C, or a combination of these effects. The aim of this study was to determine whether relative myocyte calcium levels are decreased and, if so, what the causes for this decrease might be.

The main regulator of the SR calcium load is, as mentioned above, SERCA, which pumps calcium from the cytosol into the SR, a process that is essential for the next myocyte contraction. NCX is another important sarcolemmal protein that competes with SERCA by

removing one calcium ion from the cell in exchange for three sodium ions, with the limitation that NCX has to be in forward mode as it can change direction with a positive membrane potential or high Na^+ levels in the cell. The relative contribution of SR and NCX on calcium removal from the cytosol is species dependent. In human cardiomyocytes 63% of calcium removal is achieved by SERCA and 37% by NCX. In mice, only 9% is dependent on NCX but 90% on SERCA (1% is a combined contribution of a sarcolemmal Ca^{2+} ATPase and a mitochondrial Ca^{2+} uniporter) (30). Elevated SR Ca^{2+} load is associated with increased inotropy due to higher calcium availability during contraction. An important regulator of SERCA is phospholamban. In its dephosphorylated state, it binds to SERCA and reduces calcium re-uptake, whereas in the phosphorylated form it dissociates into the cytosol. PLB has two phosphorylation sites, namely the protein kinase A (PKA, **Fig. 2**)-dependent (33) site on serine at the position 16 and the CaMKII-dependent site on threonine at the position 17 (34). Both kinases could be an off-target of sorafenib treatment leading ultimately to negative inotropy via depressed SERCA activity due to reduced PLB phosphorylation or even through reduced calcium influx caused by interactions of CaMKII with LTCC or RyR (34). Furthermore, phosphorylation of CaMKII on threonine 286 increases calmoduline binding by 1,000-fold, thus leading to higher acitivity of the kinase (34).

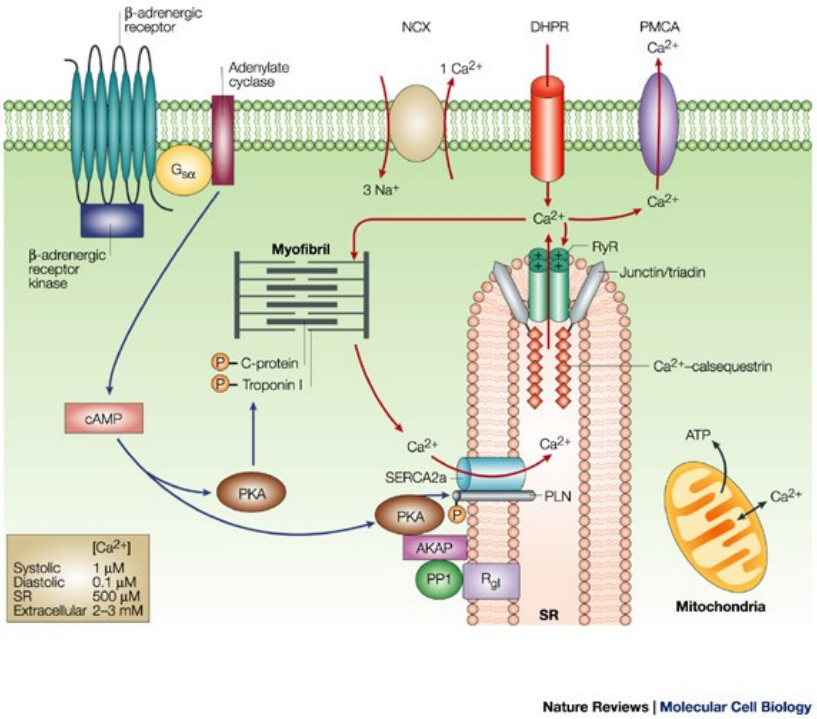

Figure 2 PKA and the role in calcium cycling. Mac Lennan et al. 2003, Nature Reviews (33)

1.4 Sorafenib

Currently, sorafenib is approved by the European Medicine Agency (EMA) and the U.S. Federal Food and Drug Administration (FDA) for the treatment of hepatocellular carcinoma, renal cell carcinoma, and differentiated thyroid carcinoma as a second line therapy.

Although developed as a Raf (rapidly accelerated fibrosarcoma) inhibitor, sorafenib (Nexavar©; BAY 43-9006; (35,36)) exhibits substantial inhibition on VEGFR-2, VEGFR-3, PDGFR-ß, Flt-3, c-kit, and p38α. Sorafenib promotes the development of acute coronary syndromes in 4.9% of patients compared to 0.4% in the placebo group and, in a second study, in 2.7% (placebo group 1.3%) [for an overview of side effects see **Table 1**] (22). Sorafenib also reduces phosphorylation of the ERK pathway in a study from Sridhar et al. 2005 (37), but 2010 Hasinoff and Patel could not reproduce this effect suggesting that cardiotoxicity of sorafenib is not caused, as previously thought, by inhibiting RAF/MEK/ERK kinase cascade but by inhibition of a different or a combination of different kinases due to the lack of selectivity (38).

Force et al. (39) consider the inhibition of Raf1 and VEGFR as the main contributors to cardiotoxicity of sorafenib. Although Raf1 kinase activity does not seem to have an effect on the unstressed heart, on the stressed heart (pressure overload) Harris et al. (40) could show protective effects. Inhibition of Raf1 causes increased cardiomyocyte apoptosis and fibrosis, and by inhibiting VEGFR capillary density was reduced leading to fibrosis and heart failure, especially in hypertensive patients (41,42).

Along the lines of multiple mechanisms involved in cardiac remodelling, including different effects like vascular remodelling, hypertrophy, fibrosis, and inflammation, the rather unspecific MTKI sorafenib may be involved in many of these processes.

Here, we sought to define acute, myocyte-intrinsic effects of the MTKI sorafenib on cardiac contractility and intracellular calcium cycling.

1.4.1 Sorafenib's effect on acute contractility in human multicellular myocardial preparations

In previous work by our laboratory (43) we assessed acute changes in myocardial contractility caused by sorafenib by exposing human atrial muscle strips to increasing concentrations of the drug and measuring the developed force.

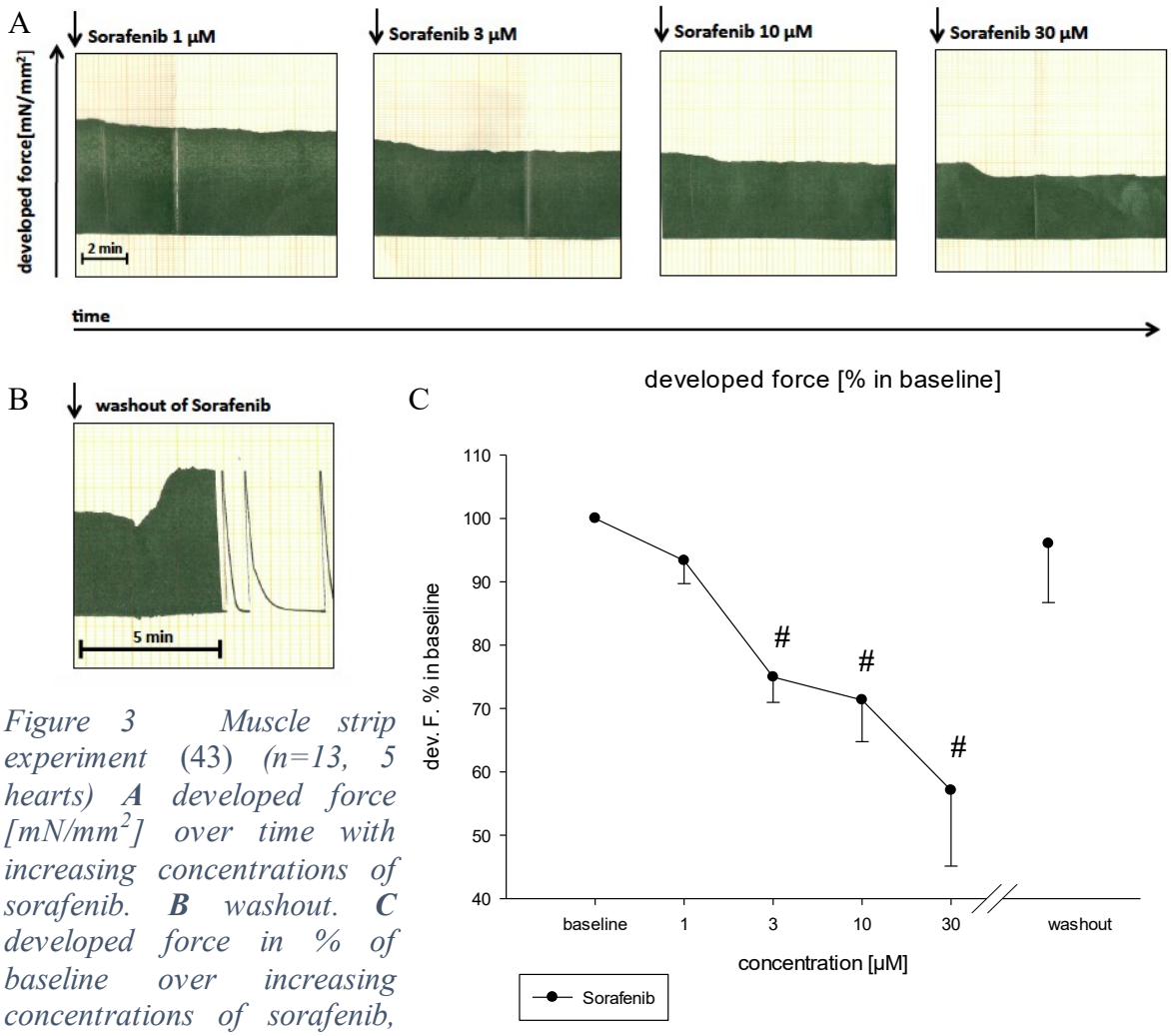

*Figure 3 Muscle strip experiment (43) (n=13, 5 hearts) **A** developed force [mN/mm^2] over time with increasing concentrations of sorafenib. **B** washout. **C** developed force in % of baseline over increasing concentrations of sorafenib, #: p<0.01 vs baseline*

Sorafenib dose-dependently and reversibly decreased cardiac contractile force (**Fig. 3**). Kinetics did not show significant alterations. This demonstrated that besides adverse cardiac effects through chronic administration that may be due to alterations of multiple cell types, sorafenib also acutely impacts cardiac inotropy. There are three main mechanisms to regulate acute cardiac contractility:

1. <u>Length-dependent regulation through Frank-Sterling mechanism and Anrep effect</u>

   Increased preload causes stretching of cardiac muscle and leads to increased activated cross-bridging (Frank-Sterling). This effect is calcium independent and instant, while the Anrep effect has a slow response and is accompanied by a gradual rise of calcium.

2. Frequency-dependent regulation through Bowditch effect

   Higher frequencies lead to higher intracellular calcium levels. The exact cause of it is yet not completely understood but stretch-activated channels (like TRPC channels) are likely involved (44).

3. Beta-adrenergic stimulation

   Post-translational regulation mainly due to PKA activation leading to the activation of a variety of different ECC proteins resulting in higher cytosolic calcium levels and myofilament calcium sensitivity. (7)

As stimulation frequency and preload (length) are constant in our set-up, increased cytosolic calcium and/or myofilament calcium sensitivity remain potential mediators of blunted contractility due to sorafenib. Previously, our group excluded alterations of myofilament calcium sensitivity as the cause of reduced inotropy (4) with the similar TKI sunitinib making alterations in calcium sensitivity unlikely as the prime reason for decreased contractility.

1.5 Hypothesis

Decreased cytoplasmic calcium transient peak amplitude underlies acute negative inotropy by sorafenib. This is caused by sorafenib-induced PTMs of major calcium cycling proteins resulting in decreased SR calcium load and slowed calcium re-uptake kinetics.

2 Methods

2.1 Calcium measurements

Ventricular cardiomyocytes were isolated from adult male C57BL/6J mice (The Jackson Laboratory, Charles River, Sulzfeld, Germany) at 12 – 25 weeks of age.

2.1.1 Isolation

2.1.1.1 Preparation

Prior to isolation, glass-bottom petri-dishes (WillCo Wells) were covered with Laminin (Sigma-Aldrich, USA) dissolved in normal Tyrode (NT) (350µg/ml) and the following solutions were prepared (**Table 2**) and the pH was adjusted to 7.40 (pH213 pH Meter, Hanna instruments) at room temperature (RT).

Table 2 Overview of solutions used for isolation

Name	*AfCS Solution Protocol N°*
Stock perfusion buffer, 1X Reagent	PS00000452
Perfusion buffer	PS00000451
Myocyte stopping buffer 1	PS00000449
Myocyte stopping buffer 2	PS00000450
Myocyte digestion buffer	PS00000447

After inducing unconsciousness with Isoflurane (0.5ml, Forane® in a specialised induction chamber), I injected 50 I.U. Heparin (Gilvasan pharma) i.p. [0,1ml Heparin diluted in 0.9ml of 0.9% NaCl solution (Fresenius)]. Approx. 15min later I anaesthetised the mouse with 1ml of isoflurane. I waited until the mouse became calm, the breathing slowed down and the reaction to a toe pinch was negative. Only then I quickly carried out cervical dislocation and removed the heart from the chest. To avoid any air embolism, I compressed all vessels to and from the heart with an anatomical forceps. Placing the heart in perfusion

solution, I gently pressed the heart against the wall to remove excess blood in the ventricles.

2.1.1.2 Cannulation, perfusion and dissociation

For cannulation and perfusion, I used a Langendorff setup (Radnoti Low Volume – High Yield Myocyte System, 120108-B) with a heating system (Lauda alpha A6) (**Fig. 4**).

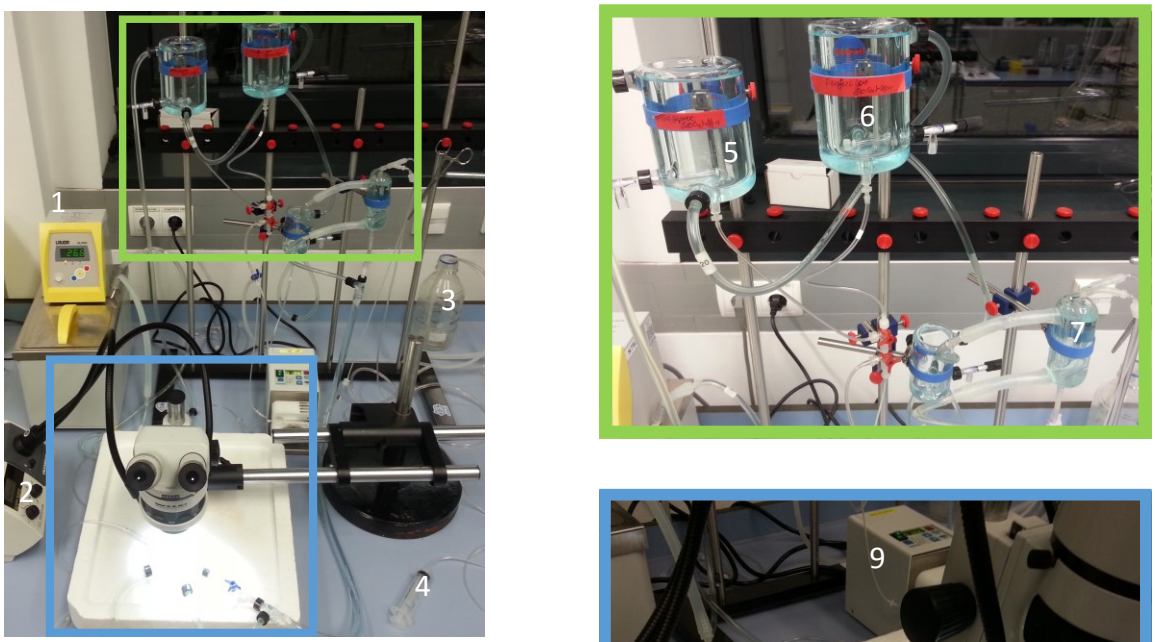

1 Heating system
2 Light system
3 Waste disposal
4 Syringe (for water level adjustment in bubble trap)
5 Enzyme solution
6 Perfusion solution
7 Bubble trap
8 Flow pump
9 Petri-dish
a solution inlet + cannula
b solution outlet
c heating

Figure 4 Workspace and setup for cannulation and perfusion

After prefilling the tubes with perfusion solution and making sure that no air bubbles had been left in the system, I cannulated the ascending aorta using two angled forceps (S&T JFA-5b TC) under a stereomicroscope (Wild Heerbrugg, M5A; light system: Olympus, KL 1600 LED). Then I fixated the heart at the cannula with a 5-0 silk suture (Ethicon) and started constant-flow perfusion (Flow pump ISM 834C, Ismatec; flow rate: 2.5ml/min, temperature: 37°C). The time required for the enzyme solution to reach the tip of the

cannula starting from the reservoir was 2.5min. During this time, the rest of the blood was washed out by perfusion solution. The enzymatic digestion was stopped after 4.5min and the ventricles were cut from the rest of the heart and placed in 'stopping solution 1' where the ventricles were further dissected into small pieces. After that, I gently resuspended the tissue using four 2.5ml Pasteur pipettes with gradually smaller opening diameters for 1min each. Then I filtrated the resulting suspension through a 250µm Nylon-mesh into a 50ml Falcon tube and allowed the cells to sediment for 10min.

2.1.1.3 Calcium reintroduction and washing of cell pellet

I removed the supernatant and added the calcium solutions in a stepwise manner with increasing Ca^{2+} concentration (0.125mM Ca^{2+} and 0.25mM Ca^{2+}) in 10 min intervals to increase the Ca^{2+} concentration to a final value of 0.5mM Ca^{2+} using 'Myocyte stopping buffer 1' for calcium dilution, each after first removing the supernatant. In the last step, I added NT (136mM NaCl, 5mM KCl, 1mM $CaCl_2$, 1mM $MgCl_2$, 10mM HEPES, 10mM Glucose; pH=7.40 at RT) with a calcium concentration of 1mM. The cells were kept in this solution for approximately 20min before the experiment.

2.1.2 Preparation for calcium measurement

2.1.2.1 Preparation of cells

I loaded the isolated cardiomyocytes with the calcium-sensitive fluorescent dye fluo-4/AM (1,5µM) (Life Technologies, USA). Fluo-4/AM has the ability to increase its fluorescence intensity over 100-fold upon calcium binding and is excited with a laser diode (488nm) with only a slight wavelength shift between the excitation and emission light (Ex/Em of Ca^{2+} - bound form 494/506 nm, **Fig. 5**).

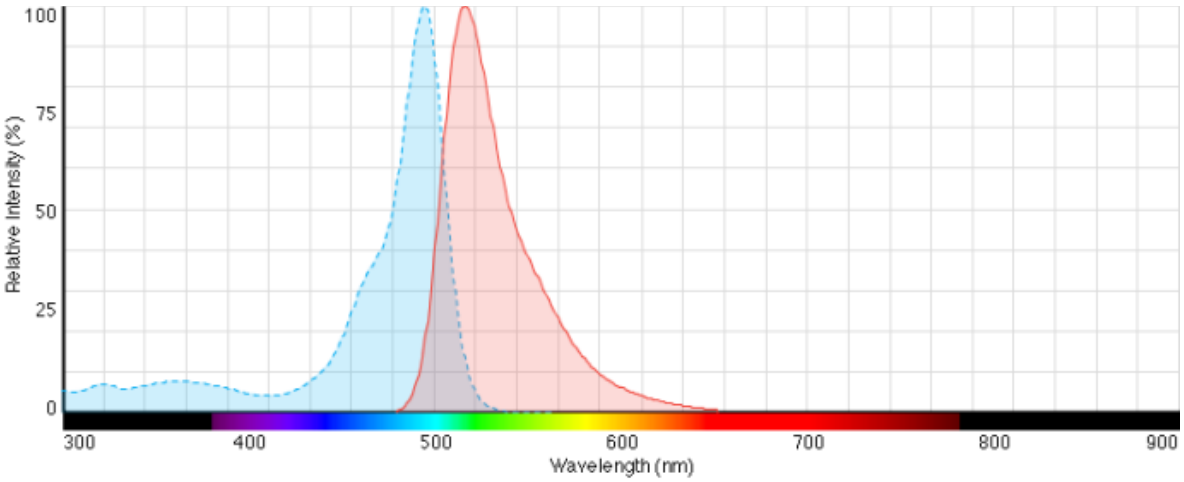

Figure 5 Fluorescent spectrum of fluo-4, AM. Blue is the bandwidth of excitation, red the bandwidth of the emission spectrum. Thermo Fisher HP (45)

Fluo-4/AM has a molecular weight of 1096.95 g/mol and has the following chemical formula and structure (**Fig. 6**):

$$C_{51}H_{50}F_2N_2O_{23}$$

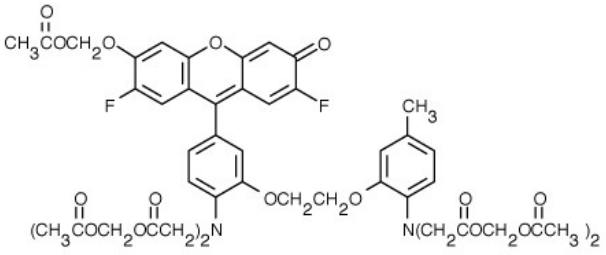

Figure 6 Molecular structure of fluo-4. Thermo Fisher HP (45)

Due to poor water solubility of fluo-4, the carboxylic acid groups of the dye are esterified to a non-fluorescent acetoxymethyl (AM) ester to make fluo-4/AM lipophilic and hence cell permeant. (45)

I dissolved the dye in 9µl dimethyl sulfoxide (DMSO, fluo-4/AM is not soluble in water) and prepared three aliquots à 3µl (corresponding to 16.67µg fluo-4/AM) and stored them at -20°C.

To enhance attachment of adult cardiomyocytes on glass-bottom petri-dishes, it is necessary to coat the dishes with laminin at least 2h before commencing the experiment. For this purpose, I diluted laminin (52.5µg) in 150µl of NT and covered each dish with approx. 35µl of the resulting solution.

After 20min in NT, I resuspended the cells and added 100µl of the suspension to 1800µl of NT in a 2ml vial (Eppendorf, covered with aluminium foil to protect fluorescently labelled cells from light). For staining, I loaded the cells with 0.56µl fluo-4/AM (corresponding to a final concentration of 1.5µM) [and 1µl pluronic acid (ThermoFisher, to facilitate the solubilisation of the dye in water)] and incubated for 20min at RT, followed by washing

the cells with 2ml NT twice for each dish. After 15min of de-esterification cells were ready for measurement.

2.1.2.2 Preparation of setup

Before starting with the measurement, I prepared six different solutions (**Table 3**) and filled the perfusion system, 25ml syringes connected to a valve controller (VC-8, Warner Instruments), with it (**Fig. 7**).

Table 3 Solutions used for CaT measurement

Solution	Concentration
1) NT	see above
2) Caffeine	30mM in NT
3) Sorafenib	10µM in NT
4) Sorafenib+ Isoproterenol	10µM + 10nM in NT
5) DMSO	0.1% in NT
6) DMSO+ Isoproterenol	0.1% + 10nM in NT

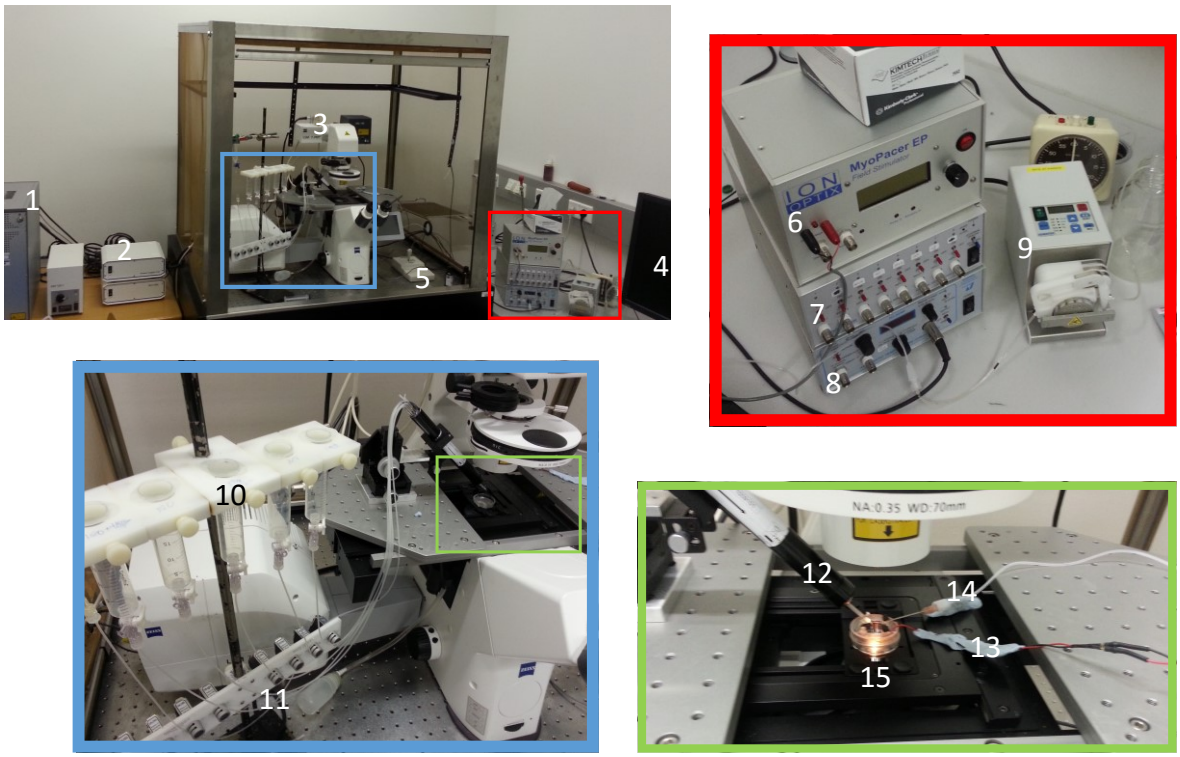

1 Light source (laser diode)
2 Power supply
3 Zeiss LSM 700
4 PC
5 Micromanipulator
6 Myopacer
7 Relay/Valve control unit
8 Temperature control unit
9 Peristaltic flow pump (siphoning)
10 Syringes filled with solutions
11 Relays/Valves
12 Heated solution outlet
13 Field electrodes
14 Siphoning inlet
15 Petri-dish (field stim.)

Figure 7 Experimental setup for CaT measurement

2.1.3 Measurement

For measurements, I used a Zeiss laser scanning microscope (LSM 700) with a 40x oil-immersion objective lens (Fluar 40x/1.30 Oil). After cells were transferred to a recording bath chamber (glass-bottom petri-dish, WillCo Wells), superfused with NT at a constant flow rate using a peristaltic pump (Ismatec, ISM597D), and paced at 0.5Hz [amplitude 10V; duration 0.5ms; Myo Pacer EP Field Stimulator (IonOptix)], they were inspected using transmission light.

Only quiescent, rod-shaped and striated cells were used for experiments. A laser [Lasos - Laser Rack LSM 700, 10mW laser diode] with a wavelength of 488nm using Zen 2009 (v5.5.0.375, Zeiss) was applied in a line-scan

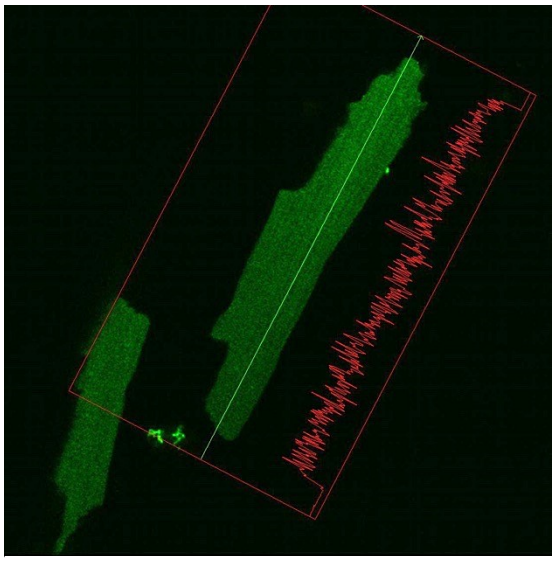

Figure 8 Cardiomyocyte under laser-microscope (dyed with fluo-4). The green line marks where measurement was done (line-scan)

mode [**Fig. 8**, 0.8% of max laser power output (80µW), pinhole max open (85.8µm section)] as indicated in the experimental protocol shown below (**Fig. 9**). At a resolution of 512 pixels the pixel size was dependent on the chosen scanning line, with a smaller pixelsize at shorter lines of interests.

Line-scan mode allows one to enhance the temporal resolution of Ca^{2+} imaging to a factor close to real-time. To reduce necessary fluo-4/AM loading concentrations and excitation intensities and thus enhance cell viability, we chose to increase pinhole size to maximum and thereby maximise detection of emitted fluorescence light (fluorescence light microscopy, high spatial resolution was not required).

I started the experiment (**Fig. 9**) by superfusing the chosen cell with NT for at least one minute to reach a steady state followed by administration of sorafenib or DMSO (control), and performing fluorescence measurements every 2 minutes. After reaching steady state again I added isoproterenol to assess beta-adrenergic response.

The protocol was concluded by switching off pacing and rapidly superfusing cells with high-dose caffeine, resulting in dumping of SR calcium to the cytosol and an ensuing high CaT as a measure of the amount of SR calcium content (**Fig. 10**). Caffeine is an activator of ryanodine receptors located in the membrane of the SR, which empties Ca^{2+} from the SR.

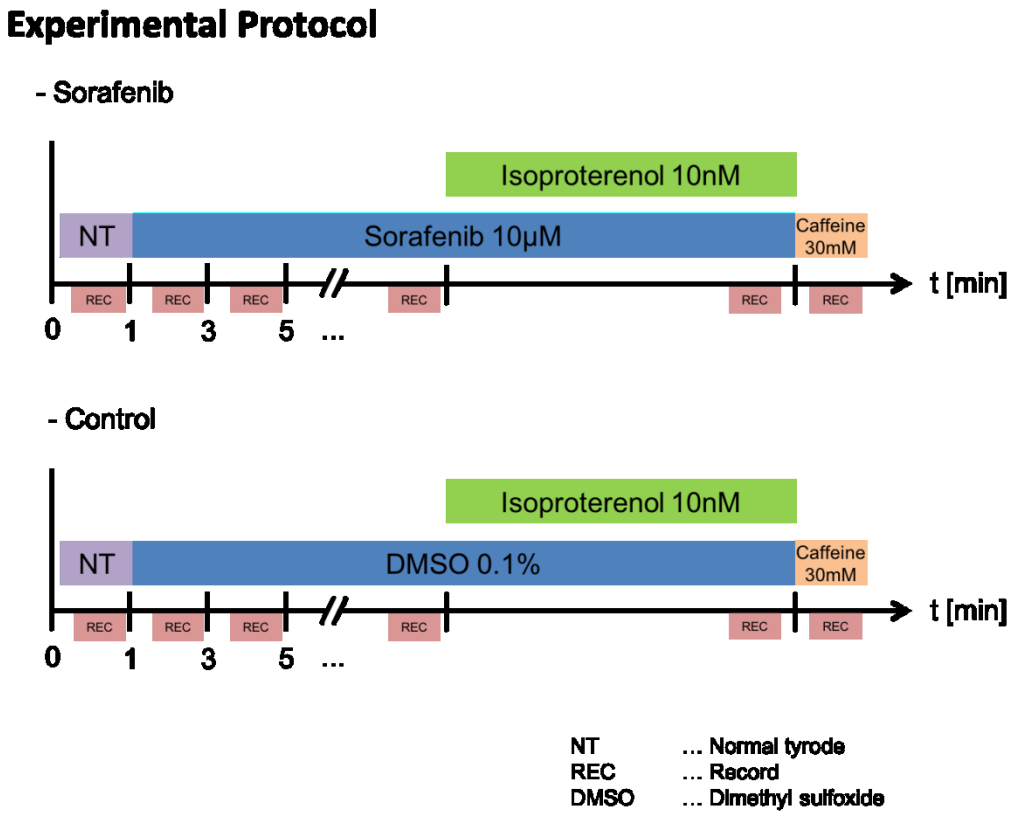

Figure 9 Experimental protocol for CaT measurement for sorafenib and control

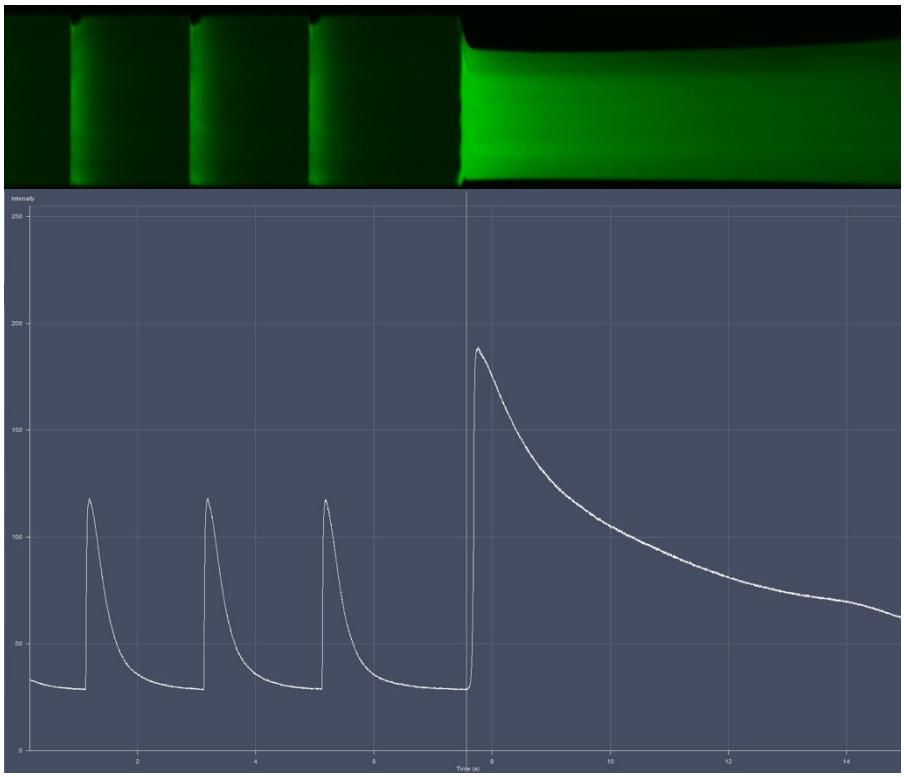

Figure 10 Caffeine-induced calcium transient (4th transient). The first three represent normal contractions under pacing (here with added isoproterenol).

2.2 Western Blot

We investigated expression and phosphorylation status of major proteins involved in cardiomyocyte calcium handling. These were phospholamban, Ca^{2+}/calmodulin-dependent protein kinase II and phosphorylated PLB on Threonine 17 and Serine 16 as well as phosphorylated CaMKII on Threonine 286.

2.2.1 Preparing cells for WB

For Western blots, I took 3 aliquots à 1.5ml of cell suspension (1 heart initially diluted in NT) after the calcium series was completed and put them into a 2ml Eppendorf tube followed by incubating them on a shaker (Sky Line DRS-12) for 14min at room temperature as shown in **Table 4**.

Table 4 Aliquots preparation for WB

Treatment	**Concentration**	**Time**
1) Sorafenib *Isoproterenol*	*10µM (≡ 1.5µl Sorafenib 10^{-2} ad 1.5ml)* *10nM (≡ 1.5µl Isoproterenol 10^{-5} ad 1.5ml)*	10min, then 4min
2) DMSO *Isoproterenol*	*0.1% (≡ 1.5µl DMSO ad 1.5ml)* *10nM (≡ 1.5µl Isoproterenol 10^{-5} ad 1.5ml)*	10min, then 4min
3) DMSO (Ctrl)	*0.1% (≡ 1.5µl DMSO ad 1.5ml)*	14min

Then I centrifuged the cells at 700g for one minute (PCV-2400, Grant-bio), removed the supernatant, and immediately snap froze the pellet in liquid nitrogen. For long-time storage, tubes were transferred to a -80°C freezer.

2.2.2 BCA – Assay

To estimate the protein concentration in each sample, necessary for WB, I prepared 7 BSA (bovine serum albumin) standards as follows:

Table 5 BSA standards

	Concentration [µg/µl]	**CLB [µl]**	**BSA stock solution [µl]**
1	blank value	500	0
2	0.5	416.5	83.5
3	1	333.3	166.7
4	1.5	250	250
5	2	166.7	333.3
6	2.5	83.5	416.5
7	3	0	500

Before using the photometer, I resuspended each sample in 100µl of ice-cold lysis buffer containing:

4475µl ddH_2O
+ 25µl PMSF [phenylmethylsulfonyl fluoride (200mM)]
+ 500µl CLB [cell lysis buffer (10x)],

followed by placing the samples in an ultrasonic ice bath 3x for 1min (Ultrasons-H., J.P. Selecta, 1200W). After another 10min on ice, I centrifuged them at 11.6k g and kept the supernatant containing the protein lysate. I pipetted all on a 96-well microplate and added 200µl of the BCA (bichinchoninic acid) working reagent (50A+1B) to each well. Photometric measurement (SPECTROstar Omega, BMG Labtech) was done after a 30min incubation period at 37°C. At a wavelength of 562nm, absorption of three different dilutions for each sample and blanks for reference purpose were measured.

Using this data, I averaged the blanks, subtracted them from the samples, and calculated the protein concentration with Microsoft Excel using a linear curve fit. Protein concentrations varied between 2.27g/l and 18.19g/l.

2.2.3 Electrophoresis

Before starting with electrophoresis (Criterion Cell, Bio-Rad; power supply: PowerPac 300 or PowerPac Basic, Bio-Rad), I prepared the samples as calculated with Excel and heated them for 5min at 95°C with a thermomixer (comfort, Eppendorf). Then I loaded 22µl of each sample – with a final protein concentration of 20µg (PLB) and 30µg (CaMKII) – and the markers into the wells. After 2.5h (20min 70V, then 2h10min 100V, RT) of electrophoresis for PLB using Tris-Tricine-Gel 16.5% (Criterion™ Precast, Bio-Rad) and 1.5h at 125V (RT) for CaMKII using Bis-Tris-Gel 4-12% (Criterion™ XT Precast, Bio-Rad), respectively, I proceeded with the transfer in a cold cabinet at 4°C. Details are shown below (**Table 6**).

2.2.4 Transfer

Transfer was done for 1h (PLB) or 2h (CaMKII) at 400mA (Criterion Blotter, Bio-Rad; power supply: PowerPac 300 or PowerPac Basic, Bio-Rad). Details are shown in **Table 6**.

2.2.5 Incubation with antibodies

Previous to the incubation period, I stained the membranes with Ponceau solution to visualise proteins for 10min and washed membranes in H_20. Then I blocked the membrane with 5% milk dissolved in TBST [(tris-buffered-saline and Tween 20 (polysorbat)] for 1h at RT, washed them twice (à 10min) with TBST, started the incubation with the primary antibody (phCaMKII and phPLB, diluted in 0.5% milk) and left it on a shaker over night at 4°C. The next day I washed the membrane again three times (à 10min, TBST) and incubated with the secondary antibody (diluted in 0.5% milk, 50min at 4°C). After that I washed it four times (à 10min, TBST) and incubated 5min with the substrate.
I repeated the whole procedure after stripping the membrane with a stripping buffer for 10min (washing 4min before and after with TBST) for total CaMKII and total PLB, respectively (after rechecking in between).

Table 6 Overview of all parameters for WB

	PLB	**CaMKII**
Gel	16.5% Tris-Tricine-Gel	4-12% Bis-Tris-Gel
Electrophoresis	2h, 125V	20min at 70V + 2h10min at 100V
Running buffer	Tris-Tricine 1:10	XT MOPS 20x diluted to 1x
Marker	All blue, Low range	All blue
Transfer	1h, 400mA	2h, 400mA
Membrane	Nitrocellulose 0.1µm (Amersham Protran, GE)	PVDF 0.45µm (Amersham Hybond, GE)
Transfer buffer	Transfer buffer (6.5mM Tris, 38.4mM Glycine) + 20%Methanol	Transfer buffer (6.5mM Tris, 38.4mM Glycine) + 20%Methanol
Primary antibodies (for Catalog# and Lot# see appendix)	- GAPDH 1:15.000 (Cell signaling) - PLB total 1:2.500 (Badrilla) - PLB phSer16 1:2.000 (Badrilla) - PLB phThr17 1:1.000 (Badrilla)	- GAPDH 1:20.000 (Cell signaling) - CaMKII total 1:500 (Cell signaling) - CaMKII phThr286 1:500 (Abcam)
Secondary antibodies		
Rabbit	GAPDH 1:10.000 phSer16, phThr17 1:5.000	GAPDH 1:10.000 total 1:5.000 phThr286 1:5.000
Mouse	total 1:5.000	
Substrate	- Clarity Western ECL (Thermo scientifc) → GAPDH, phSer16 - SuperSignal West Femto (Thermo scientific) → total, phThr17	- Clarity Western ECL (Thermo scientifc) → GAPDH, total -SuperSignal West Femto (Thermo scientific) → phThr286

2.2.6 Imaging

For imaging, I used the ChemiDoc™ Touch System (Bio-Rad). The first measurement was an automatic exposure to determine dynamic range and the second one was a colorimetric image for documentary purposes. Dependent on the intensity of the bands of the first measurement, I normally chose an exposure time of 20min (10 pictures).
To obtain numeric values for intensity, I had to choose the band I was interested in and subtracted the in-lane background (Image Lab v5.2.1 build 11, Bio-Rad).

2.3 Statistical Analysis

2.3.1 Calcium transients

For statistical analyses, I imported the text files from Zen 2009 Software from each measurement into R (RStudio v 0.99.491, packages: readxl, plyr, ggplot2, nlme, lme4, XLConnect). The first step was to smooth the transients (**Fig. 11**) by applying a linear filter on the time series (using 16 data points to average at once). Then, by overlapping at least three transients per measurement and averaging them for each time point, I obtained the parameters (**Fig. 12**). I performed a separate analysis for caffeine response and lastly a statistical analysis for CaTs and the caffeine response as well. (Two-way mixed ANOVA, post-hoc: pairwise t-test, for source code see appendix).

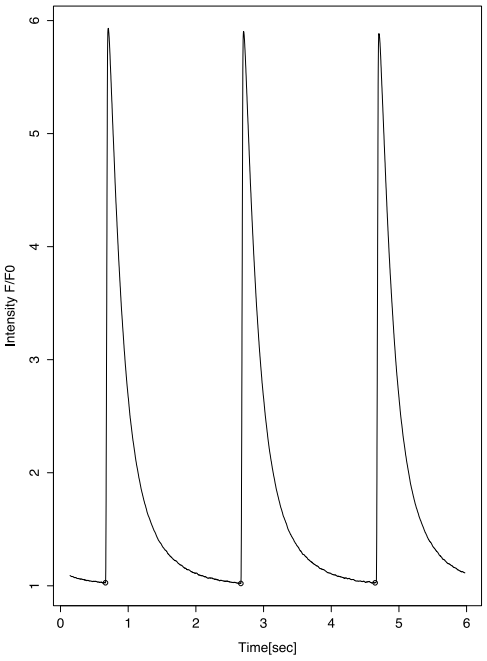

Figure 11 Smoothed transients

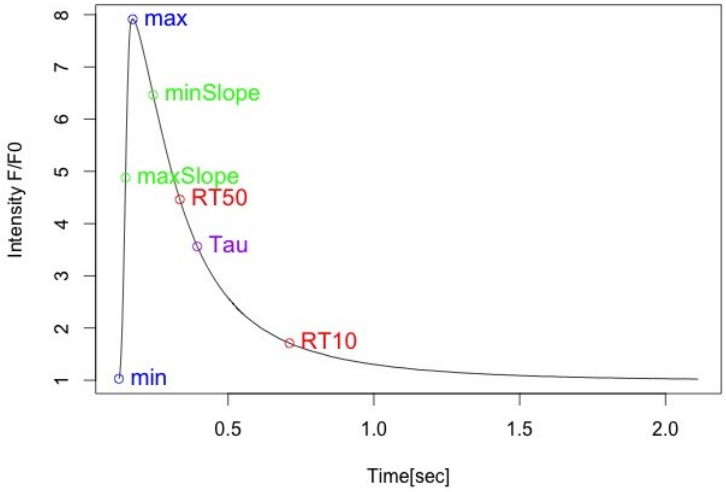

Figure 12 Averaged overlapped calcium transient with marked parameters

Figure 12 shows an averaged transient from three CaTs with all measured parameters. The amplitude was calculated by subtracting the minimal intensity of fluorescence (min) from the maximal (max) after subtracting the fluorescence background. Maximal slope (maxSlope) and minimal slope (minSlope) represents the maximal increase and decrease rate in cytoplasmic calcium. RT50, Tau, and RT10 represent the relaxation time needed to reach 50%, 1/e and 10% of the amplitude.

2.3.2 Western blots

Using the Image Lab software, I could export the data in an Excel file to normalise phPLB (serine 16 and threonine 17) to totalPLB and mean of control, phCaMKII to GAPDH and mean of control, and totalCaMKII also to GAPDH and mean of control. I imported the normalised data into R (for source code see appendix) and conducted various statistical analyses (Kruskal-Wallis rank-sum test, Friedman repeated measures ANOVA on ranks, Wilcoxon signed rank sum test, post-hoc tests: pairwise t-test or Student-Newman-Keuls test, preliminary tests: Shapiro-Wilk normality test and Bartlett test of homogeneity of variances). Data are shown as mean ± SEM. $P<0.05$ was considered statistically significant.

3 Results

All data are expressed as mean±SEM. Statistical significance was considered a p-value less than 0.05.

3.1 Cytosolic Calcium Transients

Seven murine hearts were used and isolated myocytes were randomly assigned to the Sorafenib (n=21) or control group (n=20), respectively.

3.1.1 Sorafenib-induced alterations in CaT

3.1.1.1 Calcium transient amplitude

Sorafenib treatment of cardiomyocytes resulted in a progressive decrease in calcium transient peak amplitude, which was 52±8.1% of baseline value at maximum drug effect (**Fig.13**, $p<0.001$), suggesting reduced levels of cytoplasmic calcium release from the SR during systole. However, control cells did not show any significant difference ($p=0.93$).

Analysis of the sorafenib effect revealed a time-dependent significant reduction of calcium transient amplitudes after eight minutes of treatment compared to control as shown in **Tables 7-9** and as can be seen in the following graph (**Fig. 14**).

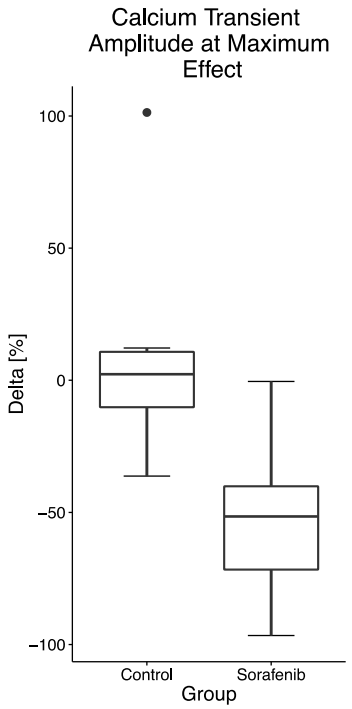

Figure 13 (right) Calcium transient peak amplitude at maximum effect; n = 17/10, p<0.001

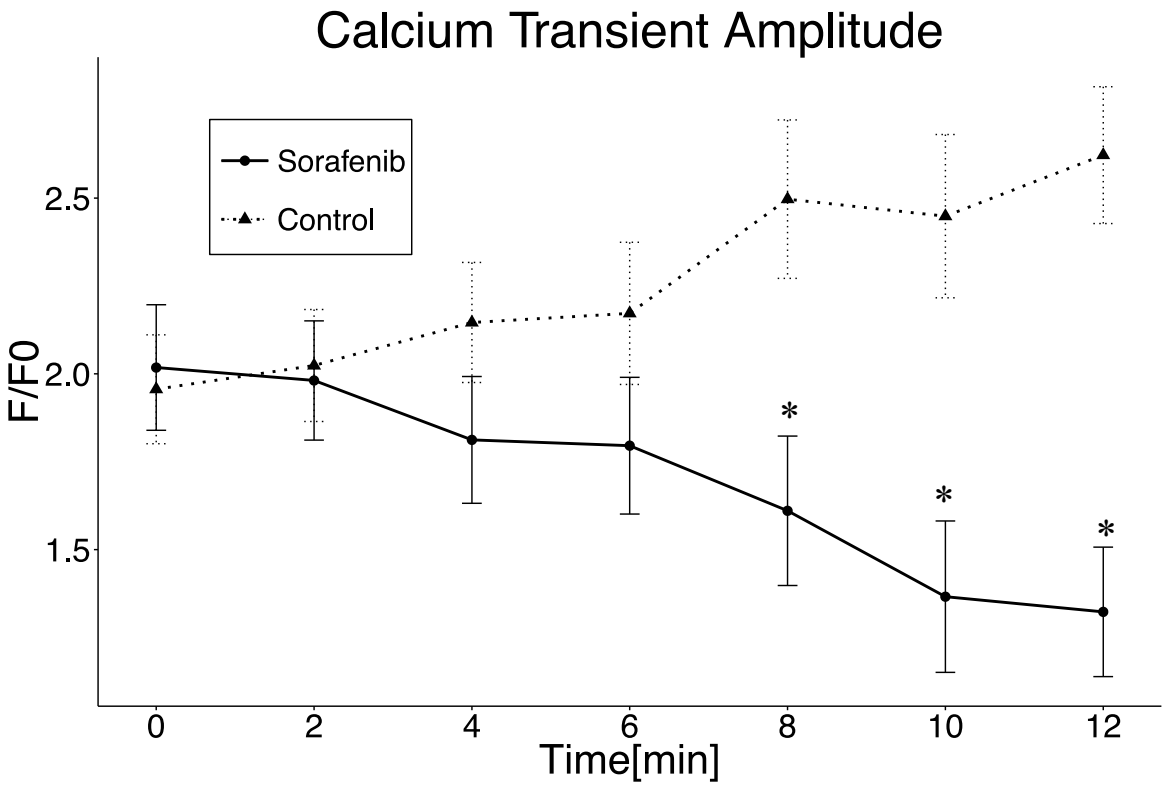

*Figure 14 Time-dependent effect of calcium transient peak amplitude in response to sorafenib treatment compared to control. *p<0.05 (compared to control; post-hoc Welch's t-test)*

3.1.1.2 Calcium cycling kinetics

Sorafenib altered several parameters of calcium cycling kinetics. The maximal slope reflects the maximal velocity of cytoplasmic calcium increase showing a significant deceleration in the treated group after six minutes compared to control while time to peak did not show any constant significant difference between groups (**Fig. 15**). The reduced slope indicates slowed calcium release, however, as calcium release velocity is also dependent on total calcium release (CaT amplitude) with reduced slope in smaller CaTs this finding must be interpreted with caution.

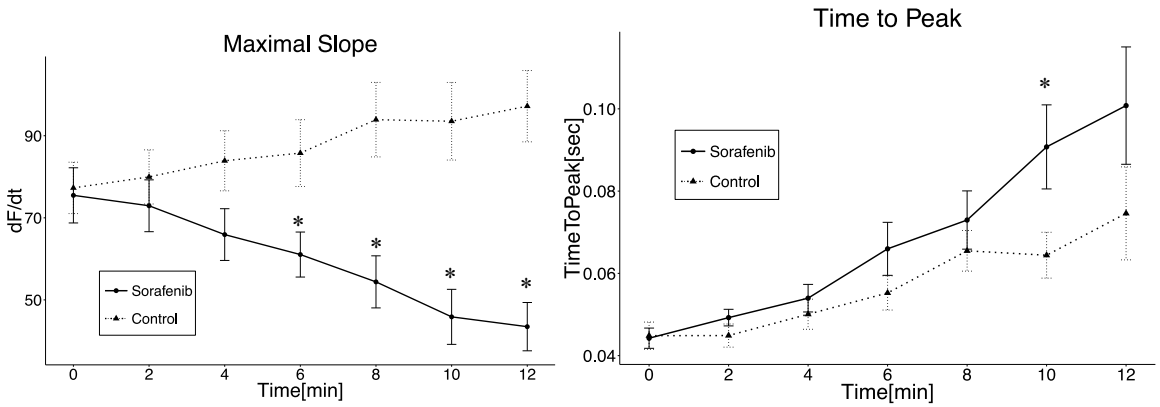

*Figure 15 left: Maximal slope under sorafenib treatment compared to control over time. right: Time to peak under sorafenib treatment compared to control over time. *p<0.05 (compared to control; post-hoc Welch's t-test)*

Ten minutes after sorafenib superfusion, RT50 was significantly prolonged in the treated group compared to control. As for RT10 and Tau, significance was already reached after eight minutes of treatment. The time at minimal CaT slope reflects the fastest time of cytosolic calcium removal. This parameter was significantly slower after eight minutes of sorafenib treatment as compared to control (**Figs. 16/17**).

These results suggest that sorafenib slowed calcium re-uptake kinetics.

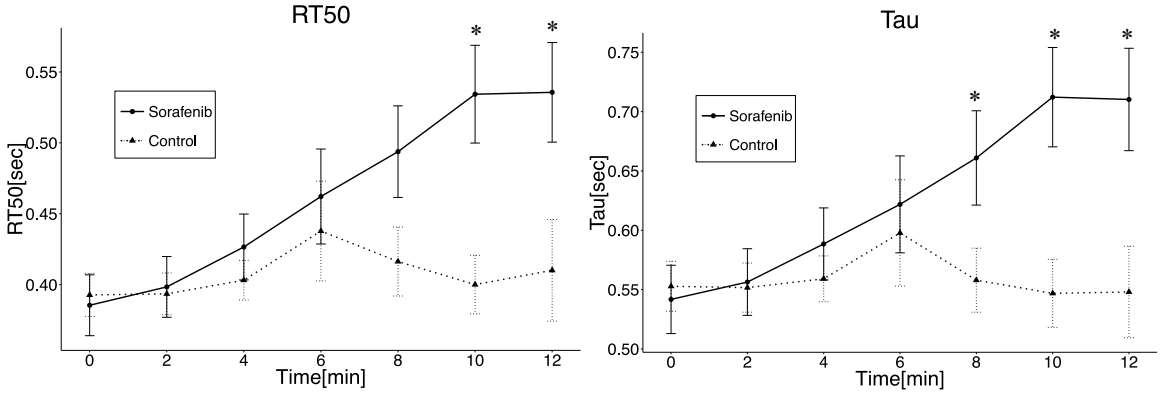

*Figure 16 left: RT50 under sorafenib treatment compared to control over time. right: Tau under sorafenib treatment compared to control over time. *p<0.05 (compared to control; post-hoc Welch's t-test)*

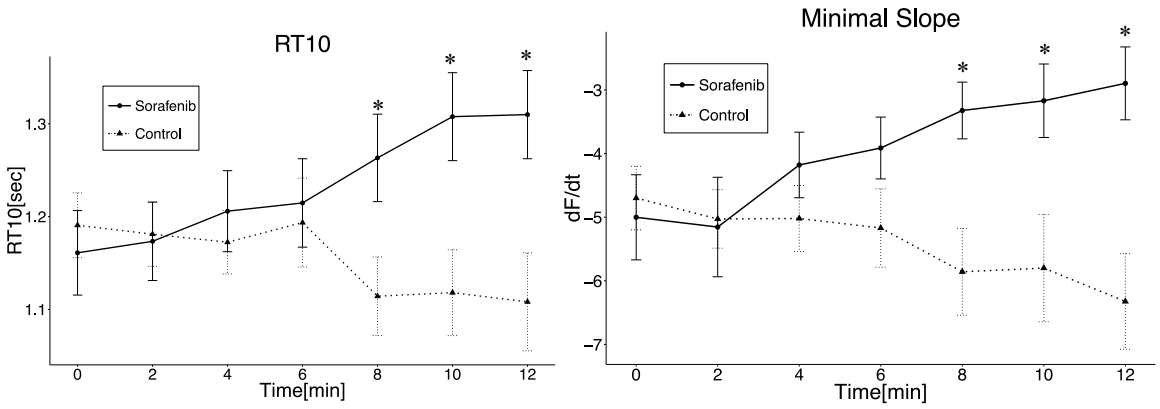

*Figure 17 left: RT10 under sorafenib treatment compared to control over time. right: Minimal slope under sorafenib treatment compared to control over time. *p<0.05 (compared to control; post-hoc Welch's t-test)*

Two-way mixed ANOVA revealed interactions between treatment and time in all studied parameters (**Table 7**). Followed by a post-hoc Welch's t-test (**Table 8**), it showed significant differences between treatment and control group. From time point eight on amplitudes were significantly reduced in the sorafenib group and calcium release and re-uptake kinetics [minimal and maximal slope, RT50 (time point ten and higher), Tau and RT10] were slowed. Maximum slope showed a significant slow-down after only six minutes of treatment. Mean values of all parameters at all time points are shown in **Table 9**.

*Table 7 2-way mixed ANOVA (sorafenib), values are p-values, *p<0.05*

	Treatment	*Time*	*Interaction (Treatment:Time)*
Amplitude	0.1716	0.0010*	<.0001*
minSlope	0.4759	0.0097*	0.0006*
maxSlope	0.0452*	<.0001*	<.0001*
RT50	0.2892	<.0001*	0.0019*
Tau	0.3367	<.0001*	0.0003*

RT10	0.5858	<.0001*	<.0001*
TimeToPeak	0.0602	<.0001*	0.0452*

*Table 8 Post-hoc Welch's t-test (sorafenib), values are p-values, *p<0.05*

Time point (min)	*0*	*2*	*4*	*6*	*8*	*10*	*12*
Amplitude	0.7954	0.8556	0.1878	0.1897	0.0083*	0.0043*	0.0005*
minSlope	0.7194	0.8901	0.2581	0.1204	0.0056*	0.0277*	0.0056*
maxSlope	0.8441	0.4458	0.0718	0.0185*	0.0018*	0.0020*	0.0009*
RT50	0.7835	0.8517	0.3950	0.6195	0.0660	0.0034*	0.0286*
Tau	0.7580	0.8926	0.4207	0.6945	0.0416*	0.0042*	0.0150*
RT10	0.6077	0.8889	0.5510	0.7564	0.0263*	0.0118*	0.0166*
TimeToPeak	0.8830	0.2164	0.4365	0.1728	0.3938	0.0356*	0.1721

*Table 9 Mean values over Time ± SEM (sorafenib), *p<0.05 vs control*

Time point	***0***	***2***	***4***	***6***	***8***	***10***	***12***
n (Ctrl/Sora)	*20/21*	*20/21*	*17/19*	*15/18*	*12/17*	*6/15*	*5/12*
Amplitude	[F/F0]						
Control	1.96±0.15	2.02±0.16	2.15±0.17	2.17±0.20	2.50±0.23	2.45±0.23	2.62±0.19
Sorafenib	2.02±0.18	1.98±0.17	1.81±0.18	1.80±0.19	1.61±0.21*	1.37±0.22*	1.32±0.18*
minSlope	[dF/dt]						
Control	-4.7±0.5	-5.0±0.5	-5.0±0.5	-5.2±0.6	-5.9±0.7	-5.8±0.8	-6.3±0.8
Sorafenib	-5.0±0.7	-5.2±0.8	-4.2±0.5	-3.9±0.5	-3.3±0.4*	-3.2±0.6*	-2.9±0.6*
maxSlope	[dF/dt]						
Control	77.3±6.3	80.0±6.6	83.9±7.3	85.8±8.1	93.9±9.1	93.5±9.5	97.2±8.7
Sorafenib	75.5±6.7	72.9±6.3	65.9±6.3	61.1±5.5*	54.4±6.3*	45.9±6.7*	43.5±5.9*

RT50	[msec]						
Control	393±15	394±15	403±14	438±35	416±24	400±21	410±36
Sorafenib	385±21	398±21	427±23	462±33	494±32	534±34*	536±35*
Tau	[msec]						
Control	553±21	552±21	559±19	598±45	558±27	547±29	548±39
Sorafenib	542±29	556±28	588±30	622±41	661±40*	712±42*	710±43*
RT10	[sec]						
Control	1.19±0.03	1.18±0.03	1.17±0.03	1.19±0.05	1.11±0.04	1.12±0.05	1.11±0.05
Sorafenib	1.16±0.05	1.17±0.04	1.21±0.04	1.21±0.05	1.26±0.05*	1.31±0.05*	1.31±0.05*
TimeToPeak	[msec]						
Control	44.9± 3.3	44.9±2.8	50.1±3.7	55.2±4.2	65.5±4.9	64.4±5.6	74.6±11.3
Sorafenib	44.2±2.5	49.2±2.0	54.0±3.3	66.0±6.4	73.0±7.1	90.8±10.2*	100.8±14.3

3.1.2 The effect of beta-adrenergic stimulation on CaT in sorafenib-treated cardiomyocytes

To test whether sorafenib interferes with the beta-adrenergic signalling pathway, isoproterenol was co-administered after reaching steady state under sorafenib treatment. Isoproterenol is a beta-1 and beta-2 receptor agonist, leading to increased cAMP levels, and thus to increased levels of PKA, which phosphorylates many ECC proteins (PLB, LTCC, RyR) and increases contractility (positive inotropy). PKA also phosphorylates myofilaments (e.g., troponin I), which enhances relaxation and therefore preserves diastolic filling at increased heart rates (30,46).

3.1.2.1 Calcium transient peak amplitude in response to isoproterenol

Mean calcium transient peak amplitude was significantly higher in the control group compared to sorafenib-treated cells, which showed an attenuated response to isoproterenol (n =15/5 cells, 7 hearts, $p < 0.001$), suggesting lower beta-adrenergic reserve (**Tables 10-12**, **Fig. 18**). In control cells, CaT peak amplitude after isoproterenol administration was amplified 3.6-fold while the same concentration of isoproterenol increased CaT amplitude only 2.7-fold (starting from a lower baseline amplitude).

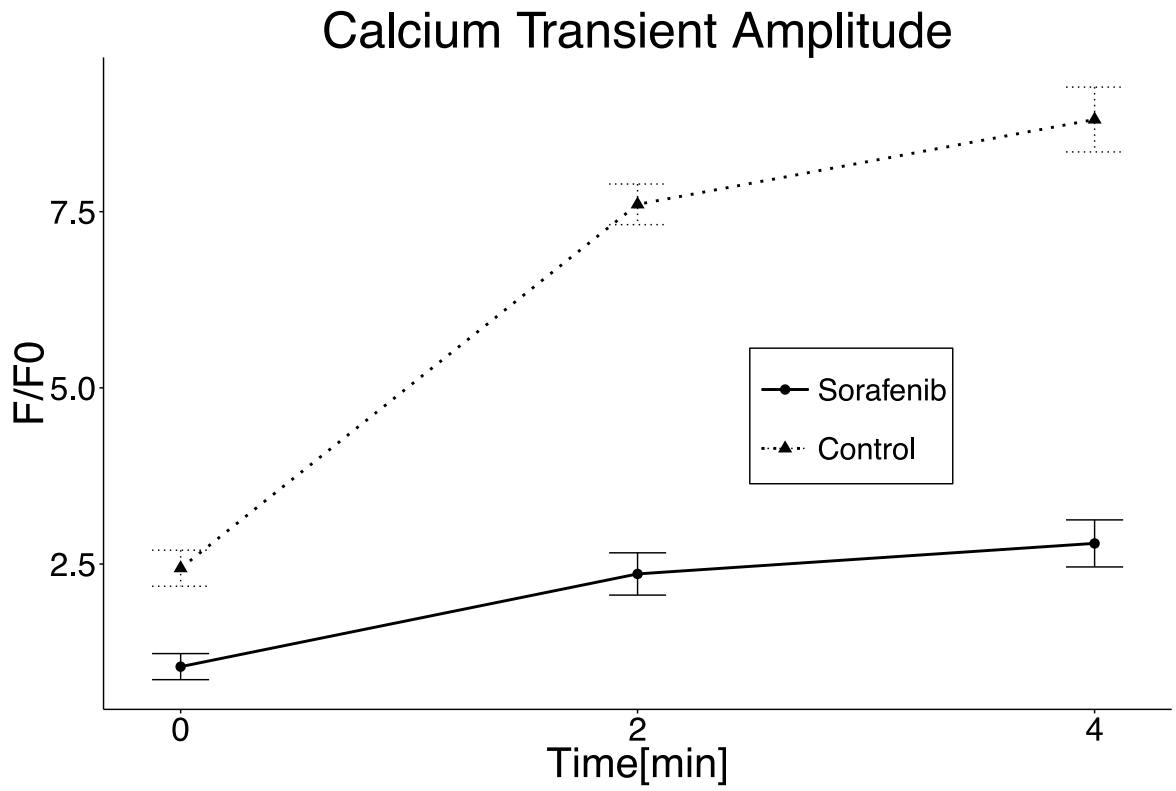

Figure 18 Calcium transient amplitude under sorafenib treatment compared to control over time (+isoproterenol superfusion). At all time points: p<0.05 (compared to control; post-hoc Welch's t-test)

3.1.2.2 Calcium cycling kinetics under isoproterenol influence

The interaction of maximal slope with treatment was significant and time to peak was not (**Fig. 19**). As mentioned before, as effects on amplitude alone can explain parts of the kinetic changes, results have to be interpreted with care.

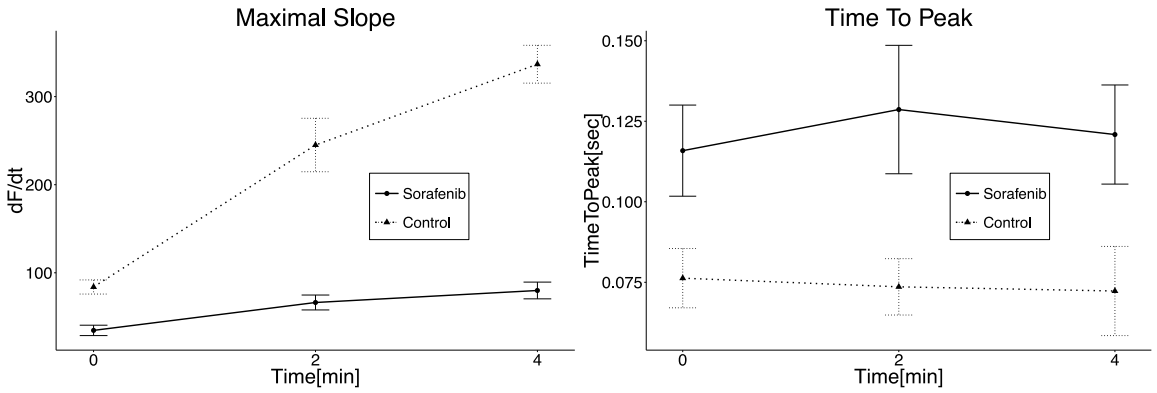

Figure 19 left: Maximal slope under sorafenib treatment compared to control over time (+isoproterenol superfusion). right: Time to peak under sorafenib treatment compared to control over time (+isoproterenol superfusion). At all time points: p<0.05 (compared to control; post-hoc Welch's t-test)

Except for minimal slope, calcium removal parameters showed no significant differences between groups over time (**Figs. 20/21**). Changes were concordant, suggesting that sorafenib did not cause major interferences in calcium re-uptake under isoproterenol influence. Minimal slope changes were only minor due to significantly lower increase in amplitudes compared to control.

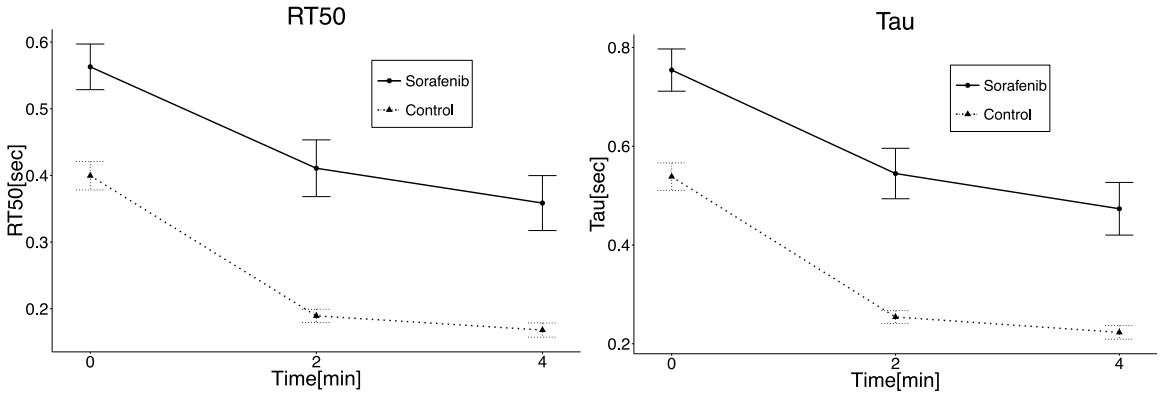

Figure 20 left: RT50 under sorafenib treatment compared to control over time (+isoproterenol superfusion). right: Tau under sorafenib treatment compared to control over time (+isoproterenol superfusion). At all time points: p<0.05 (compared to control; post-hoc Welch's t-test)

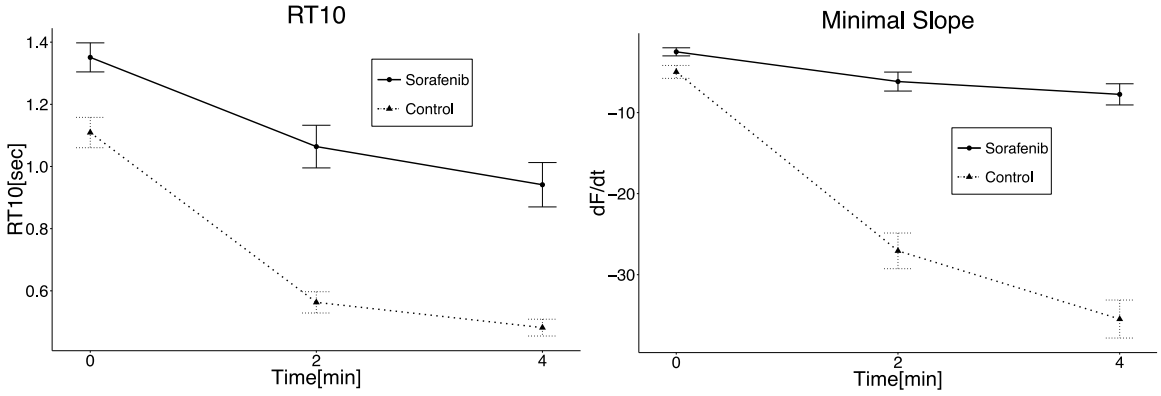

Figure 21 left: RT10 under sorafenib treatment compared to control over time (+isoproterenol superfusion). right: Minimal slope under sorafenib treatment compared to control over time (+isoproterenol superfusion). At all time points: p<0.05 (compared to control; post-hoc Welch's t-test)

Two-way mixed ANOVA (**Table 10**) revealed interactions between treatment and time only for amplitude and minimal and maximal slope. The remaining parameters did not show any significant interactions, except for RT10, which showed a trend toward significance. Post-hoc Welch's t-test (**Table 11**) revealed significant differences at all time

points for all parameters. However, the lack of significant interactions (RT50, Tau, RT10, Time to peak) has to be kept in mind. Mean values of all parameters at all time points are shown in **Table 12**.

*Table 10 2-way mixed ANOVA (sorafenib+isoproterenol), values are p-values, *p<0.05*

	Treatment	*Time*	*Interaction (Treatment:Time)*
Amplitude	<.0001*	<.0001*	<.0001*
minSlope	<.0001*	<.0001*	<.0001*
maxSlope	<.0001*	<.0001*	<.0001*
RT50	0.0088*	<.0001*	0.6829
Tau	0.0057*	<.0001*	0.6732
RT10	0.0011*	<.0001*	0.0633
TimeToPeak	0.0924	0.3857	0.6176

*Table 11 Post-hoc Welch's t-test (sorafenib+isoproterenol), values are p-values, *p<0.05*

Time point	*0*	*2*	*4*
Amplitude	0.0018*	<.0001*	0.0002*
minSlope	0.0320*	0.0001*	0.0011*
maxSlope	0.0009*	0.0027*	0.0021*
RT50	0.0008*	<.0001*	0.0004*
Tau	0.0005*	<.0001*	0.0004*
RT10	0.0038*	<.0001*	<.0001*
TimeToPeak	0.0310*	0.0220*	0.0461*

*Table 12 Mean values over Time ± SEM (sorafenib+isoproterenol), *p<0.05 vs control*

Time point	*0*	*2*	*4*
n (Ctrl/Sora)	*5/15*	*5/14*	*3/15*
Amplitude	[F/F0]		
Control	2.44±0.26	7.60±0.29	8.81±0.46
Sorafenib	1.04±0.18*	2.36±0.30*	2.80±0.33*
minSlope	[dF/dt]		
Control	-4.9±0.8	-27.1±2.2	-35.5±2.3
Sorafenib	-2.5±0.5*	-6.2±1.2*	-7.7±1.3*
maxSlope	[dF/dt]		
Control	83.9±8.0	245.1±30.3	336.8±21.5
Sorafenib	34.6±5.9*	66.3±8.5*	79.9±9.5*
RT50	[msec]		
Control	400±21	189±10	168±11
Sorafenib	563±34*	411±43*	359±41*
Tau	[msec]		
Control	538±28	254±13	223±14
Sorafenib	754±43*	545±51*	473±53*
RT10	[sec]		
Control	1.11±0.05	0.56±0.03	0.48±0.03
Sorafenib	1.35±0.05*	1.06±0.07*	0.94±0.07*
TimeToPeak	[msec]		
Control	76.3± 9.2	73.6±8.8	72.3±13.8
Sorafenib	115.9±14.1*	128.6±19.9*	120.9±15.4*

3.1.3 Assessment of SR calcium content

After assessment of sorafenib effects on CaT at rest and after isoproterenol administration we assessed SR calcium content by caffeine-induced rapid opening of RyR. This leads to complete depletion of SR, thereby allowing assessment of the total amount of calcium in the SR and the percentage of calcium released during normal twitch (=fractional release, **Fig. 23 B**).

Here, we found a significantly lower SR calcium content in sorafenib-treated cells compared to control cells (n=10/3 cells, from 5 and 3 hearts, respectively; $p<0.01$, **Fig. 22**).

An exponential curve fit using Excel to calculate tau of the caffeine transients revealed borderline significant differences between sorafenib compared to control (t-test; p=0.063).

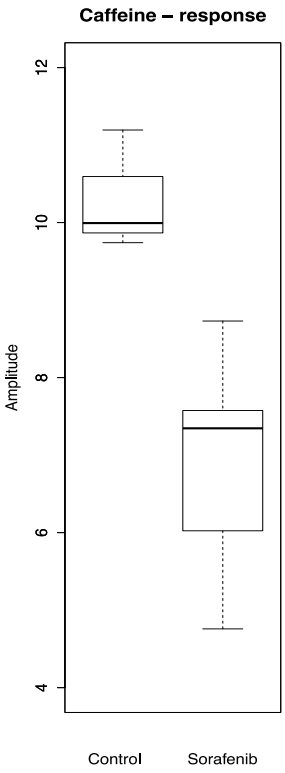

Figure 22 Caffeine response; n=10/3, p<0.01

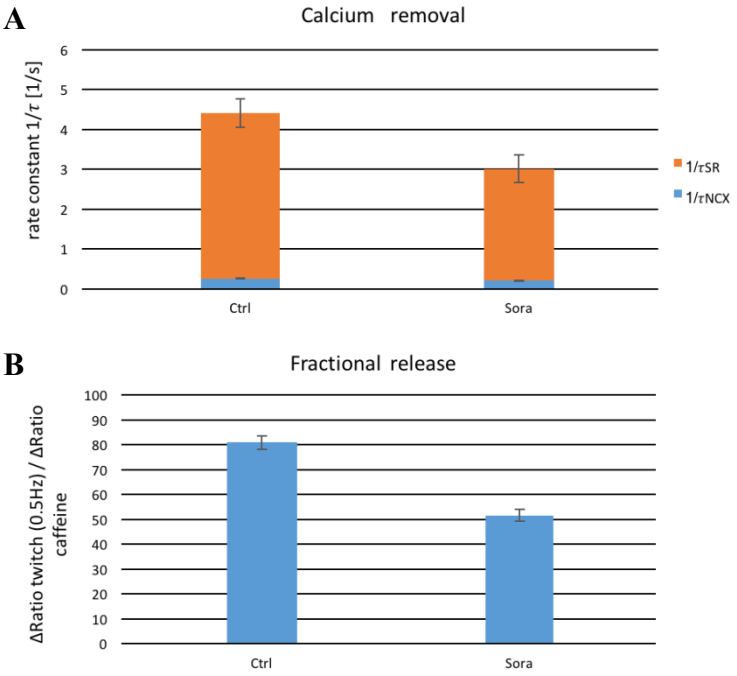

Figure 23 Calcium removal (A) and fractional release (B) calculated following Tocchetti et al. (47)

Calcium removal and fractional release was impaired in the Sorafenib group [calculated following Tocchetti et al (47); $\frac{1}{\tau_{twitch}} = \frac{1}{\tau_{NCX}} + \frac{1}{\tau_{SR}}$, $\tau_{NCX} = \tau$ of caffeine decline].

Relative contribution (**Fig. 23, A**) of SR to calcium removal decreased from 94.1% to 93.1% (4.16±0.34 to 2.81±0.36 s^{-1}, p=0.043 vs control) in sorafenib treated cells. Vice versa, relative contribution of NCX increased from 5.9% to 6.9% (0.26±0.01 to 0.21±0.01 s^{-1}, borderline significance: p=0.059 vs control), respectively. Fractional release (**Fig. 23**,

B) was markedly reduced in sorafenib-treated cells, accounting for 51.6±2.4% as compared to 81.0±2.7% in the control group.

These results indicate that sorafenib-induced reduction of calcium transient peak amplitude is due to decreased SR calcium content and SR Ca^{2+} release.

3.2 Phosphorylation Status of Calcium Cycling Proteins

3.2.1 Phospholamban

PLB is a regulator of SERCA activity. It has two phosphorylation sites. Increased phosphorylation on either of these sites increases SERCA pump activity leading to higher calcium concentration in the SR. Administration of sorafenib reduced phosphorylation of PLB at Serine 16 as shown in **Figs. 24/25**. Threonine 17 phosphorylation was slightly reduced (**Fig. 26**).

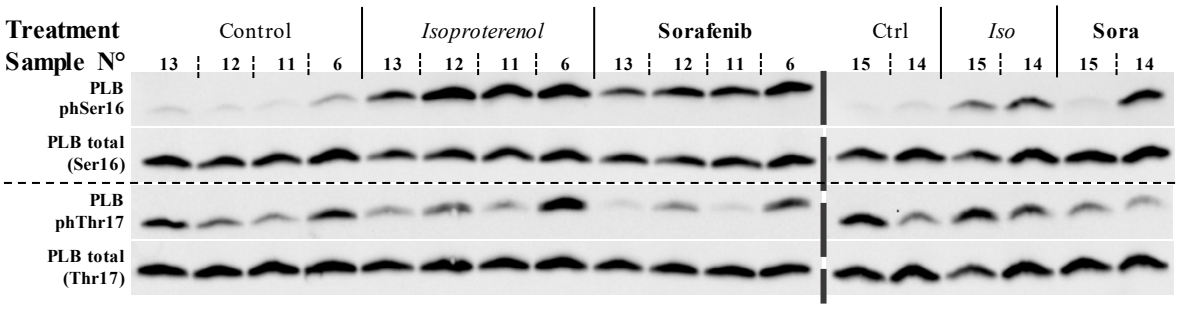

Figure 24 WB of PLB (total and the two phosphorylation sites)

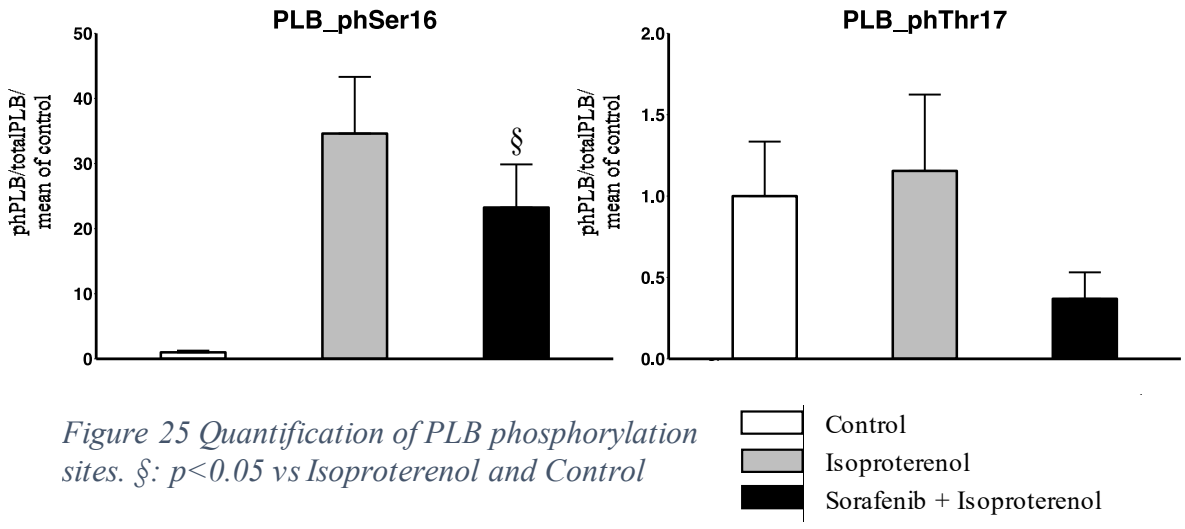

Figure 25 Quantification of PLB phosphorylation sites. §: p<0.05 vs Isoproterenol and Control

Due to the lack of homoscedasticity and non-normality we performed a Kruskal-Wallis rank-sum test and post-hoc paired t-tests:

*Table 13 Kruskal-Wallis rank sum-test and post-hoc paired t-tests for PLB, *p<0.05*

Kruskal-Wallis rank-sum test	χ^2	*df*	*p-value*
phSerine16	8.64	2	0.013*
phThreonine17	4.64	2	0.098

PLB_phSer16

paired t-test	*Control*	*Isoproterenol*
Isoproterenol	0.02*	-
Iso+Sorafenib	0.02*	0.03*

PLB_phThr17

paired t-test	*Control*	*Isoproterenol*
Isoproterenol	0.60	-
Iso+Sorafenib	0.13	0.13

Although phosphorylation-changes due to treatment at threonine 17 are not significant in the Kruskal-Wallis test, if we assume paired samples using Friedman repeated measures ANOVA on ranks it is (p=0.002, **Table 14**). Followed by a pairwise multiple comparison of ranks, treatment with sorafenib+isoproterenol resulted in a significantly lower phosphorylation at threonine 17 compared to control or isoproterenol (**Table 14**).

*Table 14 Friedman test and post-hoc Student-Newman-Keuls test for PLB_phThr17, *p<0.05*

Friedman RM ANOVA on Ranks	χ^2	*df*	*p-value*
phThreonine17	10.33	2	0.002*

Pairwise Multiple Comparison of Ranks (Student-Newman-Keuls)	*Control*	*Isoproterenol*
Isoproterenol	p>0.05	-
Iso+Sorafenib	p<0.05*	p<0.05*

If we compare phosphorylation at threonine 17 between the isoproterenol and sorafenib + isoproterenol groups, sorafenib significantly reduces threonine 17 phosphorylation (Wilcoxon signed rank test: Z=-2.201, p=0.031, **Table 15**).

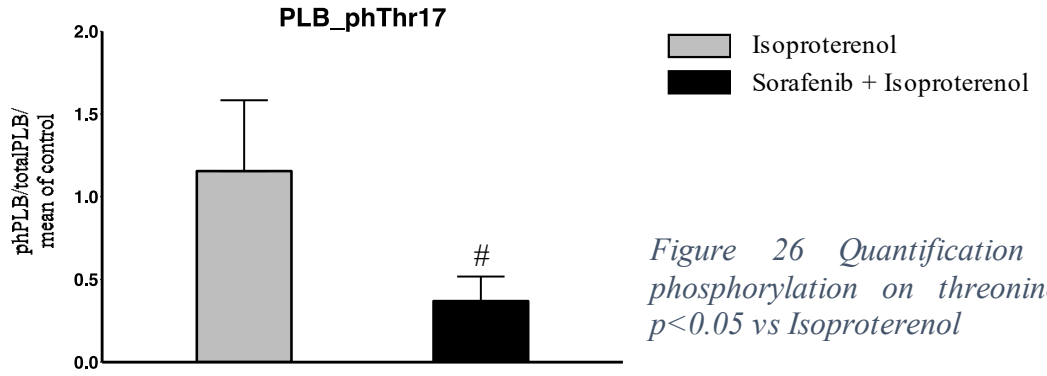

Figure 26 Quantification of PLB phosphorylation on threonine 17. #: p<0.05 vs Isoproterenol

*Table 15 Wilcoxon signed rank sum test for PLB_phThr17 between isoproterenol and sorafenib+isoproterenol, *p<0.05*

Wilcoxon Signed Rank Test	*Z (based on pos. ranks)*	*p-value*
phThreonine17	-2.201	0.031*

The results of phosphorylation at threonine 17 have to be interpreted with care due to the relatively small sample size and the fact that isoproterenol does not directly stimulate phosphorylation at threonine 17, therefore reducing power of tests which compare differences in all three groups.

3.2.2 Ca^{2+}/calmodulin-dependent protein kinase II

CaMKII increases SR calcium levels by phosphorylating threonine 17 on PLB or by interacting with LTCC or RyR. The performed WB for CaMKII phosphorylated on threonine 286 showed no significant difference to control (**Figs. 27/28**).

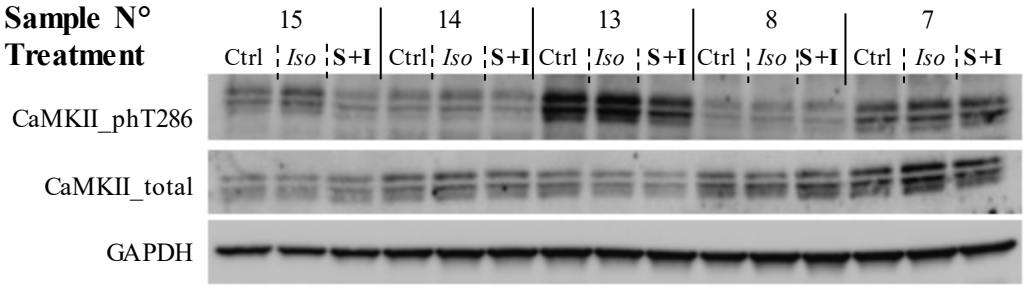

Figure 27 WB of CaMKII (total, one phosphorylation site, and GAPDH)

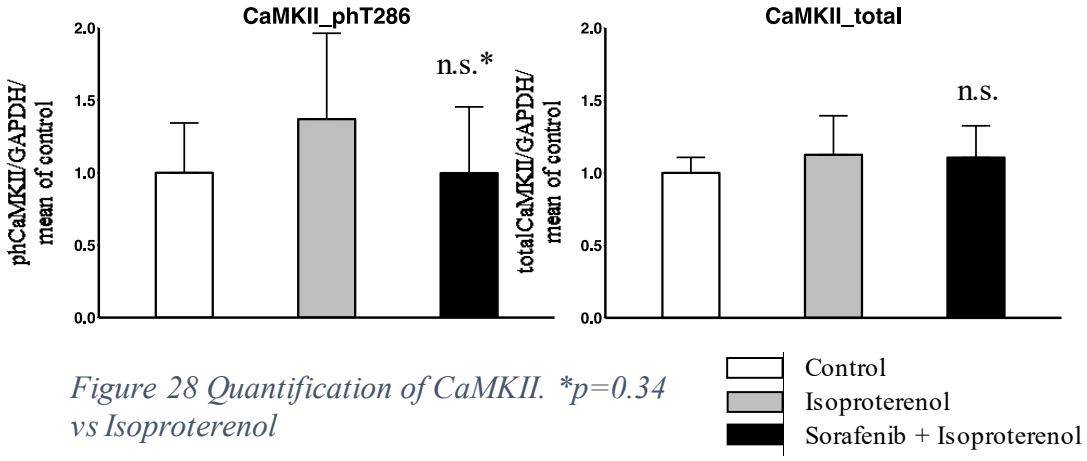

*Figure 28 Quantification of CaMKII. *p=0.34 vs Isoproterenol*

4 Discussion

Sorafenib significantly decreased intracellular CaT peak amplitudes compared to the control group beginning at eight minutes after administration. This is in line with negative inotropy observed in human multicellular myocardial preparations observed in previous experiments. Moreover, almost all of the kinetic parameters of ECC were negatively affected. Tau, RT10, and RT50 were prolonged and slopes became flatter, whereas time to peak showed minor changes. These results indicate that sorafenib affects calcium removal kinetics probably due to interference with SERCA (main contributor to CaT amplitude decline in mice, 90% of total removal) and/or NCX (9% of total removal) because all relaxation times were prolonged indicating slowed re-uptake of calcium into the SR via SERCA and/or efflux of calcium via NCX. Plasma membrane Ca^{2+} ATPase (PMCA) or the mitochondrial calcium uniporter play a negligible role at room temperature (48).

Isoproterenol increased CaT peak amplitudes and this response was attenuated in the presence of sorafenib. Slopes (CaT kinetics) also became steeper with only slight changes in the treatment group. Time constant changes, however, did not show any significant differences between the two groups, decreasing almost to the same extent (albeit starting from different values) with only RT10 showing borderline significant difference.

Caffeine administration revealed a significantly decreased SR calcium content (30,49). Calculated fractional release and calcium removal (following Tocchetti et al. (47)) evidenced lower calcium levels in SR under sorafenib treatment. The relative contribution of SR to calcium removal marginally (not statistically significant) decreased from 94.1% to 93.1% and relative NCX contribution increased from 5.9% to 6.9%. Overall, sorafenib slightly altered NCX activity increasing Tau by 23.5% from 3.9 to 4.8 seconds. As assessment of SERCA and NCX activity derived from caffeine transients is indirect and relies on several assumptions, these results need to be interpreted with care, particularly given the differences in CaT amplitude and kinetics prior to administration of caffeine.

Western blots showed significantly reduced phosphorylation at serine 16 and a trend towards reduced phosphorylation at threonine 17 in sorafenib-treated cardiomyocytes. Serine 16 and threonine 17 are the phosphorylation sites for PKA and CaMKII, respectively. These data suggest that sorafenib reduces PKA-dependent phosphorylation of PLB. CaMKII activity, assessed by autophosphorylation site at threonine 286, did not show significant differences between groups in line with only minor changes in threonine 17 phosphorylation of PLB.

Our results demonstrate that changes in acute myocardial contractility due to sorafenib are a result of reduced PKA-dependent phosphorylation of PLB leading to reduced SR calcium content, decreased CaT peak amplitudes, and blunted response to beta-adrenergic stimulation.

SERCA (ATPase at SR in **Fig. 29**) is inhibited by PLB in its dephosphorylated state, decreasing the effectiveness of calcium pumping into the SR. By inhibiting phosphorylation of PLB either through direct inhibition or through inhibition of PKA or CaMKII, PLB impairs SERCA function causing reduced SR calcium load and therefore decreased CaT amplitudes. Furthermore, an impaired function of SERCA is also consistent with slowed cytoplasmic calcium removal resulting in slower time constants.

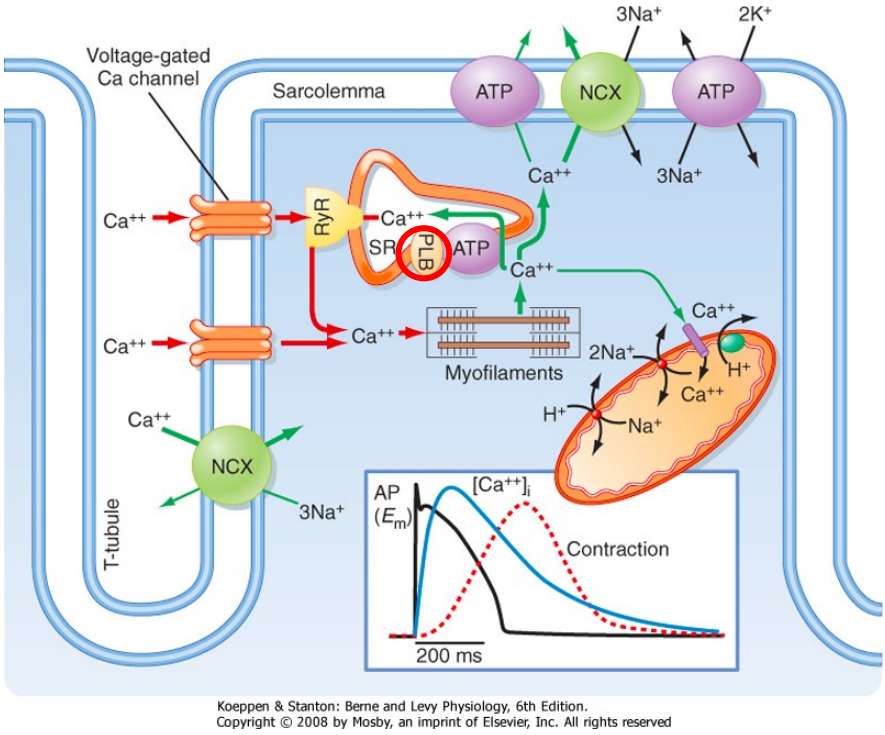

Figure 29 Schematics of calcium cycling. PLB as one probable cause for negative inotropy caused by sorafenib is marked with a red circle. Adapted from Berne and Levy Physiology, Koeppen and Stanton (50)

In a study by Duran et al. (51) , who exposed infarcted mice to high doses of sorafenib (up to 50 µM), sorafenib cardiotoxicity was shown to result in increased necrosis at high concentrations (10 and 50 µM). Duran et al. also assessed fractional shortening (FS) and CaTs of murine cardiomyocytes after long time exposure (12-48 hours) with lower (1 and 5 µM) sorafenib concentrations and did not find alterations of FS and CaTs at these concentrations. In our own work, we have consistently found negative inotropy in human

tissue and reduced CaTs at 10µM in mouse cardiomyocytes. In contrast to Duran et al., we investigated only acute effects and not chronic long time exposure. According to our work and Duran's study one may speculate that there might be a threshold between 5µM and 10µM below which no acutely detectable changes in calcium homeostasis occur. Nevertheless, we were able to show significant (acute) negative inotropic effects already at 3µM leading us to the conclusion that, if such a threshold exists, it must be below 3µM, which is lower than average plasma concentration in treated patients (52–55). A recent study from Cheng et al. supports our findings as they showed that the median lethal dose (LD_{50}) for sorafenib in human induced pluripotent stem cell derived cardiomyocytes (hiPSC-CMs) is 3.4µM (56). As mentioned above, Force et al. (39) suggest a combination of Raf1 and VEGFR inhibition as causative factors for cardiotoxicity. Interestingly, VEGFR inhibition has been shown to reduce cardiac contractility (57) and to induce cardiomyocyte death (58) in embryonic zebrafish and is assumed to contribute to normal and pathological regulation of contractility in the human heart (57). Taken together, it is likely that sorafenib cardiotoxic effects present a combination of direct and indirect as well as acute and chronic effects on several cell types.

4.1 Limitations

Because almost all (99.5%) sorafenib binds to plasma proteins (52,59), the precise concentration of sorafenib in cardiomyocytes or the interstitial fluid is not known. In addition, cell permeability of a drug can be altered by transport proteins (60). Currently, we could only identify one study (61) measuring sorafenib tissue concentration in the liver of rabbits, which is not directly comparable as the route of administration is different. Mean tissue concentrations peaked at 7.6µM in liver tumour and at 1.6µM in non-tumorous liver tissue while the average peak plasma concentration reached 126.0µM after transcatheter arterial chemoembolisation (TACE, 3mg/kg). This also does not take different compartments, like interstitial fluid, cells, and organelles into account, in which the drug could be distributed differently (62). Therefore, it remains unclear which concentration acts on the myocyte. Hence, in addition to taking published serum concentrations into account, we performed dose-response curves to determine sorafenib concentrations that impact cardiac contractility.

Secondly, albeit humans share over 95% of the genome with mice (63), there are noteworthy differences in cardiac physiology. One example is the distribution of potassium-ion-channel variants in the heart, leading to altered effects of drugs (64,65) or the contribution of SR and NCX on the cytoplasmic calcium removal. As mentioned above, SR is responsible for 90% of it in mice, whereas SR accounts for only 63% of removal in humans (30).

Furthermore, enzymatic myocyte isolation itself may have altered membrane function and activity, and staining with fluo-4 influences cellular function, as non-stained cells survived much longer and are more likely to respond to external pacing with contractions.

Arrhythmogenicity and cell death were a substantial problem in prolonged measurements, which occurred in both groups, generating a potential biased myocyte cohort. However, these limitations are method-inherent and apply to both sorafenib and control groups.

Theoretically, effects caused by PLB phosphorylation changes and reduced inotropy could be treated by sensitising myofilaments to calcium. Levosimendan is such a sensitising compound, already being in use in acute heart failure (66,67). Long-term effects are not well studied but a 2011 study described positive effects of long-term oral treatment (68) and a study on SERCA2 (SERCA isoform) knockout mice showed improved contractility and relaxation (69). This is especially interesting because of impaired SERCA activity, which also appears to be present in sorafenib treatment. However, currently levosimendan is reserved to terminal decompensated heart failure and needs repeated intravenous administration and therefore is no viable option. Attempts to increase PKA activity (reduced phosphorylation of serine 16 on PLB), e.g. by phosphodiesterase-inhibitors like milrinone (70), are also not viable options as activation of adrenergic signalling is deleterious in chronic heart failure. Another possibility might be stimulators of SERCA such as istaroxime, a non-glycoside N^+/K^+-ATPase inhibitor that has been shown to stimulate SERCA2a (71).

Moreover, one has to keep in mind that the acute effects of TKIs on cardiac contractility do not reflect cardiotoxic effects of chronic exposure that likely consist of an integration of different effects on many different cell types. In addition, unlike with conventional chemotherapy, reduction of cardiac contractility is often reversible with novel cancer therapies. Thus, stopping therapy seems a viable option. Of course, depending on the underlying cancer, this needs to take cost-benefit into account. Another option may be co-pharmacotherapy, particularly in individuals with enhanced risk of cardiac side effects (e.g.

those that already suffer from pre-existing cardiac conditions). For example, beta blockers may reduce cardiotoxic effects of trastuzumab and may even increase anti-tumour activity (72–74).

Duran's study, where increased sorafenib-induced myocyte cell death after myocardial infarction was studied, demonstrated that administering metoprolol (51) reduced cell death, hence beta blockers may also be useful for the treatment of cardiotoxic TKI side effects, even if reduced cAMP-PKA-PLB signalling is present in sorafenib's acute effects on contractility.

> *"Just as so-called precision medicine has revolutionized cancer treatment, a similar personalized approach must be incorporated in toxicity assessment in drug selection."* (13)

The best way, however, of minimising side effects would be the redesign of the drug itself.

> *"If one can identify the mechanisms of cardiotoxicity of a specific KI, the compound could be redesigned to avoid the target."* (27)

Of course, in the case of anticancer therapies, it is necessary to trade off efficacy against adverse events. This is true for both conventional chemotherapies as well as novel approaches.

We hope that with this study we can contribute to a better understanding of the side effects of the drug leading ultimately to improved safety and quality of life of patients.

5 References

1. Yaish, P., Gazit, A., Gilon, C. & Levitzki, A. Blocking of EGF-dependent cell proliferation by EGF receptor kinase inhibitors. *Science (80-.).* **242,** (1988).
2. Shelburne, N. *et al.* Cancer treatment-related cardiotoxicity: Current state of knowledge and future research priorities. *J. Natl. Cancer Inst.* **106,** dju232- (2014).
3. Schmidinger, M. *et al.* Cardiac toxicity of sunitinib and sorafenib in patients with metastatic renal cell carcinoma. *J. Clin. Oncol.* **26,** 5204–5212 (2008).
4. Rainer, P. P. *et al.* Sunitinib causes dose-dependent negative functional effects on myocardium and cardiomyocytes. *BJU Int.* **110,** 1455–1462 (2012).
5. Arora, a & Scholar, E. M. Role of tyrosine kinase inhibitors in cancer therapy. *J Pharmacol Exp Ther* **315,** 971–979 (2005).
6. Agnetti, G., Husberg, C. & Eyk, J. E. Van. Divide and Conquer - The Application of Organelle Proteomics to Heart Failure. *Circ. Res.* **108,** 512–526 (2011).
7. Hill, J. A. & Olsen, E. N. *Muscle - Fundamental Biology and Mechanisms of Disease*. (2012).
8. Natoli, C., Perrucci, B., Perrotti, F., Falchi, L. & Iacobelli, S. Tyrosine Kinase Inhibitors. *Curr. Cancer Drug Targets* **10,** 462–483 (2010).
9. Cadena, D. L. & Gill, G. N. Receptor tyrosine kinases. *FASEB J.* **6,** 2332–2337 (1992).
10. Neet, K. & Hunter, T. Vertebrate non-receptor protein-tyrosine kinase families. *Genes to Cells* **1,** 147–169 (1996).
11. Ghoreschi, K., Laurence, A. & O'Shea, J. J. Janus kinases in immune cell signaling. *Immunol. Rev.* **228,** 273–287 (2009).
12. Finn, R. S. *et al.* Dasatinib, an orally active small molecule inhibitor of both the src and abl kinases, selectively inhibits growth of basal-type/'triple-negative' breast cancer cell lines growing in vitro. *Breast Cancer Res. Treat.* **105,** 319–326 (2007).
13. Moslehi, J. J. Cardiovascular Toxic Effects of Targeted Cancer Therapies. *N. Engl. J. Med.* **375,** 1457–1467 (2016).
14. Roskoski, R. A historical overview of protein kinases and their targeted small molecule inhibitors. *Pharmacol. Res.* **100,** 1–23 (2015).
15. Hartmann, J. T., Haap, M., Kopp, H.-G. & Lipp, H.-P. Tyrosine kinase inhibitors - a review on pharmacology, metabolism and side effects. *Curr. Drug Metab.* **10,** 470–81 (2009).

16. Krause, D. S. & Van Etten, R. A. Tyrosine Kinases as Targets for Cancer Therapy. *N. Engl. J. Med.* **353,** 172–187 (2005).
17. Broekman, F., Giovannetti, E. & Godefridus, J. P. Tyrosine kinase inhibitors: Multi-targeted or single-targeted? *World J. Clin. Oncol.* **2,** 80 (2011).
18. Jabbour, E., Kantarjian, H. & Cortes, J. Use of second- and third-generation tyrosine kinase inhibitors in the treatment of chronic myeloid leukemia: An evolving treatment paradigm. *Clin. Lymphoma, Myeloma Leuk.* **15,** 323–334 (2015).
19. Soverini, S., Rosti, G., Iacobucci, I., Baccarani, M. & Martinelli, G. Choosing the best second-line tyrosine kinase inhibitor in imatinib-resistant chronic myeloid leukemia patients harboring Bcr-Abl kinase domain mutations: how reliable is the IC_{50}? *Oncologist* **16,** 868–76 (2011).
20. Stasi, I. & Cappuzzo, F. Second generation tyrosine kinase inhibitors for the treatment of metastatic non-small-cell lung cancer. *Transl. Respir. Med.* **2,** 2 (2014).
21. Caldemeyer, L., Dugan, M., Edwards, J. & Akard, L. Long-Term Side Effects of Tyrosine Kinase Inhibitors in Chronic Myeloid Leukemia. *Curr. Hematol. Malig. Rep.* **11,** 71–79 (2016).
22. Bayer. Product information Nexavar. 1–30
23. Berardi, R. *et al.* State of the art for cardiotoxicity due to chemotherapy and to targeted therapies: A literature review. *Crit. Rev. Oncol. Hematol.* **88,** 75–86 (2013).
24. Yeh, E. T. H. & Bickford, C. L. Cardiovascular Complications of Cancer Therapy. *J. Am. Coll. Cardiol.* **53,** 2231–2247 (2009).
25. Hall, P. S., Harshman, L. C., Srinivas, S. & Witteles, R. M. The Frequency and Severity of Cardiovascular Toxicity From Targeted Therapy in Advanced Renal Cell Carcinoma Patients. *JACC Hear. Fail.* **1,** 72–78 (2013).
26. Srikanthan, A. *et al.* Cardiovascular toxicity of multi-tyrosine kinase inhibitors in advanced solid tumors: A population-based observational study. *PLoS One* **10,** 1–14 (2015).
27. Cheng, H. & Force, T. Why do Kinase Inhibitors Cause Cardiotoxicity and What can be Done About It? *Prog. Cardiovasc. Dis.* **53,** 114–120 (2010).
28. Hedhli, N. & Russell, K. S. Cardiotoxicity of molecularly targeted agents. *Curr. Cardiol. Rev.* **7,** 221–33 (2011).
29. Marks, A. R. Cardiac Intracellular Calcium Release Channels. *Circ. Res.* **87,** (2000).
30. Bers, D. M. *Excitation-Contraction Coupling and Cardiac Contractile Force (Second Edition)*. (Springer Netherlands, 2001). doi:10.1007/978-94-010-0658-3

31. Bers, D. M. Cardiac excitation-contraction coupling. *Nature* **415,** 198–205 (2002).
32. Klabunde, R. E. Cardiovascular Physiology Concepts. Available at: http://www.cvphysiology.com/. (Accessed: 12th February 2017)
33. MacLennan, D. H., Kranias, E. G. & Best, C. H. PHOSPHOLAMBAN : A CRUCIAL REGULATOR OF CARDIAC CONTRACTILITY. *Nat. Rev. Mol. Cell Biol.* **4,** 566–577 (2003).
34. Grueter, C. E., Colbran, R. J. & Anderson, M. E. CaMKII, an emerging molecular driver for calcium homeostasis, arrhythmias, and cardiac dysfunction. *J. Mol. Med.* **85,** 5–14 (2007).
35. Wilhelm, S. M. *et al.* BAY 43-9006 Exhibits Broad Spectrum Oral Antitumor Activity and Targets the RAF/MEK/ERK Pathway and Receptor Tyrosine Kinases Involved in Tumor Progression and Angiogenesis. *Cancer Res.* **64,** 7099–7109 (2004).
36. Wilhelm, S. *et al.* Discovery and development of sorafenib: a multikinase inhibitor for treating cancer. *Nat. Rev. Drug Discov.* **5,** 835–844 (2006).
37. Sridhar, S. S., Hedley, D. & Siu, L. L. Raf kinase as a target for anticancer therapeutics. *Mol. Cancer Ther.* **4,** (2005).
38. Hasinoff, B. B. & Patel, D. Mechanisms of Myocyte Cytotoxicity Induced by the Multikinase Inhibitor Sorafenib. *Cardiovasc. Toxicol.* **10,** 1–8 (2010).
39. Force, T., Krause, D. S. & Van Etten, R. A. Molecular mechanisms of cardiotoxicity of tyrosine kinase inhibition. *Nat. Rev. Cancer* **7,** 332–44 (2007).
40. Harris, I. S. *et al.* Raf-1 kinase is required for cardiac hypertrophy and cardiomyocyte survival in response to pressure overload. *Circulation* **110,** 718–723 (2004).
41. Shiojima, I. *et al.* Disruption of coordinated cardiac hypertrophy and angiogenesis contributes to the transition to heart failure. *J. Clin. Invest.* **115,** 2108–18 (2005).
42. Izumiya, Y. *et al.* Vascular endothelial growth factor blockade promotes the transition from compensatory cardiac hypertrophy to failure in response to pressure overload. *Hypertens. (Dallas, Tex. 1979)* **47,** 887–93 (2006).
43. Wallner, M., von Lewinski, D., Pichler, M. & Rainer, P. P. *Muscle strip experiment - sorafenib*. (2016).
44. Seo, K. *et al.* Hyperactive Adverse Mechanical Stress Responses in Dystrophic Heart Are Coupled to Transient Receptor Potential Canonical 6 and Blocked by cGMP–Protein Kinase G ModulationNovelty and Significance. *Circ. Res.* **114,**

(2014).

45. Fluo-4, AM, cell permeant - Thermo Fisher Scientific. Available at: https://www.thermofisher.com/order/catalog/product/F14201. (Accessed: 19th January 2017)
46. Chen, P. P., Patel, J. R., Rybakova, I. N., Walker, J. W. & Moss, R. L. Protein kinase A–induced myofilament desensitization to Ca^{2+} as a result of phosphorylation of cardiac myosin–binding protein C. *J. Gen. Physiol.* **136,** 615–627 (2010).
47. Tocchetti, C. G. *et al.* Nitroxyl improves cellular heart function by directly enhancing cardiac sarcoplasmic reticulum Ca2+ cycling. *Circ. Res.* **100,** 96–104 (2007).
48. Mackiewicz, U. & Lewartowski, B. Temperature dependent contribution of Ca2+ transporters to relaxation in cardiac myocytes: Important role of sarcolemmal Ca 2+-ATPase. *J. Physiol. Pharmacol.* **57,** 3–15 (2006).
49. Kong, H. *et al.* Caffeine induces Ca2+ release by reducing the threshold for luminal Ca2+ activation of the ryanodine receptor. *Biochem. J.* **414,** 441–52 (2008).
50. Koeppen, B. M. & Stanton, B. A. *Berne & Levy Physiology*. (2010).
51. Duran, J. M. *et al.* Sorafenib cardiotoxicity increases mortality after myocardial infarction. *Circ. Res.* **114,** 1700–1712 (2014).
52. Blanchet, B. *et al. Validation of an HPLC-UV method for sorafenib determination in human plasma and application to cancer patients in routine clinical practice*. *Journal of Pharmaceutical and Biomedical Analysis* **49,** (2009).
53. Tod, M. *et al.* Functional and clinical evidence of the influence of sorafenib binding to albumin on sorafenib disposition in adult cancer patients. *Pharm. Res.* **28,** 3199–3207 (2011).
54. Fucile, C. *et al.* Measurement of sorafenib plasma concentration by high-performance liquid chromatography in patients with advanced hepatocellular carcinoma: is it useful the application in clinical practice? A pilot study. *Med. Oncol.* **32,** 335 (2015).
55. Abou-Alfa, G. K. *et al.* Phase II study of sorafenib in patients with advanced hepatocellular carcinoma. *J. Clin. Oncol.* **24,** 4293–4300 (2006).
56. Sharma, A. *et al.* High-throughput screening of tyrosine kinase inhibitor cardiotoxicity with human induced pluripotent stem cells. *Sci. Transl. Med.* **9,** (2017).

57. Rottbauer, W. *et al.* VEGF-PLC 1 pathway controls cardiac contractility in the embryonic heart. *Genes Dev*. **19,** 1624–1634 (2005).
58. Cheng, H. *et al.* A novel preclinical strategy for identifying cardiotoxic kinase inhibitors and mechanisms of cardiotoxicity. *Circ. Res.* **109,** 1401–1409 (2011).
59. EMA. Nexavar - Product information. 1–6 (2010).
60. Muller, P. Y. & Milton, M. N. The determination and interpretation of the therapeutic index in drug development. *Nat. Rev. Drug Discov*. **11,** 751–761 (2012).
61. Parvinian, A., Casadaban, L. C., Hauck, Z. Z., van Breemen, R. B. & Gaba, R. C. Pharmacokinetic study of conventional sorafenib chemoembolization in a rabbit VX2 liver tumor model. *Diagn. Interv. Radiol.* **21,** 235–40 (2015).
62. Mouton, J. W. *et al.* Tissue concentrations: do we ever learn? *J. Antimicrob. Chemother.* **61,** 235–7 (2008).
63. Why mouse genetics? Available at: https://www.jax.org/genetics-and-healthcare/genetics-and-genomics/why-mouse-genetics.
64. Fedorov, V. V. *et al.* Effects of KATP channel openers diazoxide and pinacidil in coronary-perfused atria and ventricles from failing and non-failing human hearts. *J. Mol. Cell. Cardiol.* **51,** 215–225 (2011).
65. Glukhov, A. V., Flagg, T. P., Fedorov, V. V., Efimov, I. R. & Nichols, C. G. Differential KATP channel pharmacology in intact mouse heart. *J. Mol. Cell. Cardiol.* **48,** 152–160 (2010).
66. Nieminen, M. S. *et al.* Levosimendan: current data, clinical use and future development. *Hear. lung Vessel.* **5,** 227–45 (2013).
67. Kasikcioglu, H. A. & Cam, N. A review of levosimendan in the treatment of heart failure. *Vasc. Health Risk Manag.* **2,** 389–400 (2006).
68. Jalanko, M., Kivikko, M., Harjola, V.-P., Nieminen, M. S. & Laine, M. Oral levosimendan improves filling pressure and systolic function during long-term treatment. *Scand. Cardiovasc. J.* **45,** 91–97 (2011).
69. Hillestad, V. *et al.* Long-term levosimendan treatment improves systolic function and myocardial relaxation in mice with cardiomyocyte-specific disruption of the Serca2 gene. *J. Appl. Physiol.* **115,** (2013).
70. Packer, M. *et al.* Effect of Oral Milrinone on Mortality in Severe Chronic Heart Failure. *N. Engl. J. Med.* **325,** 1468–1475 (1991).
71. Shah, S. J. *et al.* Effects of istaroxime on diastolic stiffness in acute heart failure syndromes: Results from the Hemodynamic, Echocardiographic, and

Neurohormonal Effects of Istaroxime, a Novel Intravenous Inotropic and Lusitropic Agent: A Randomized Controlled Trial in P. *Am. Heart J.* **157,** 1035–1041 (2009).

72. Seicean, S. *et al.* Cardioprotective Effect of -Adrenoceptor Blockade in Patients With Breast Cancer Undergoing Chemotherapy: Follow-Up Study of Heart Failure. *Circ. Hear. Fail.* **6,** 420–426 (2013).
73. Pituskin, E. *et al.* Multidisciplinary Approach to Novel Therapies in Cardio-Oncology Research (MANTICORE 101-Breast): A Randomized Trial for the Prevention of Trastuzumab-Associated Cardiotoxicity. [Epub ahead of print]. *J. Clin. Oncol.* JCO2016687830 (2016).
74. Gulati, G. *et al.* Prevention of cardiac dysfunction during adjuvant breast cancer therapy (PRADA): a 2 × 2 factorial, randomized, placebo-controlled, double-blind clinical trial of candesartan and metoprolol. *Eur. Heart J.* **37,** 1671–1680 (2016).
75. Blay, J.-Y. A decade of tyrosine kinase inhibitor therapy: Historical and current perspectives on targeted therapy for GIST. *Cancer Treat. Rev.* **37,** 373–384 (2011).

Appendix

Transient and Caffeine Response Analysis

```
#Transient analysis
overlap <- function() {

  filename <- file.choose()
  data <- read.csv(filename, header=T, sep='\t')
  name <- basename(filename)

   Transient <- data$Intensity.Region.1 - mean(data$Intensity.Region.2,
na.rm=T)
   Time <- data$Time..s.

   #F/F0
   F0 <- min(Transient)
   Transient = Transient/F0

   #filtering
   x <- filter(Transient, rep(1,16)/16)
   y <- Time
   sensitivity <- 0.6  # 0.6 (0.97 for caff) /change only if err

    i = 61
    j = 1
    h = 0
    dummy = 2
    max = NROW(x)
    valleyarray <- array(1:10)
    timearray <- array(1:10)
    position <- array(1:10)

    plot(Time, x,type='l', xlab="Time[sec]", ylab="Intensity F/F0")
    timearray[1]=10

    #find valley
    while((max-61)>i) {
      if(x[i]<x[i-10] & x[i]<x[i+10] & x[i]<(sensitivity*x[i+45])){


        if((y[i]-timearray[dummy-1]) < 0.1) {
          valleyarray[dummy-1] = x[i]
          timearray[dummy-1] = y[i]
          position[dummy-1] = i
        }
        else {
          valleyarray[dummy] = x[i]
          timearray[dummy] = y[i]
          position[dummy] = i
          dummy = dummy+1
```

```
        h=h+1
      }
      i = i+1
    }
    else {
      i = i+1
    }
  }

  while(j<dummy) {
    points(timearray[j],valleyarray[j])
    j=j+1
  }
  l=1
  k=1

  m<-array(rep(0,position[2]-position[1]))

  while(l<(position[2]-position[1])-1)
  {
    while(k<=h) #k<= h+1 if incl last transient
    {
      m[l] <- (m[l] + x[position[k]+l])
      k = k+1
    }
    k=1
    l=l+1
  }

  m = m/h
  m[is.na(m)] <- 0
  x <- x[ x != 19 ] # remove elements with value=19
  m <- m[m!=0]      # remove elements with value=0

  plot(Time[1:NROW(m)],m,type='l', xlab="Time[sec]", ylab="Intensity F
/F0")

  # get max position
  t1 <- which(m == max(m))
  if(NROW(t1)>1){t <- t1[1]}   # check for 2 or more max
  else {t <- t1}

  points(y[t],max(m), col='blue')
  text(y[t],max(m),col='blue',labels='max',cex=1.2,pos=4)
  points(y[1],m[1], col='blue')
  text(y[1],m[1],col='blue',labels='min',cex=1.2,pos=4)

  # RT50 RT90  ->  after peak

  e<- which.max(m)
  n<- tail(m, NROW(m)-e)  # only dec
  r<- which.min(abs(n-(0.5*(max(n)-min(n))+min(n))))
  a<- which.min(abs(n-(0.1*(max(n)-min(n))+min(n))))
  r=r+e # add points to max
```

```
    a=a+e
    points(y[r], m[r], col='red')
    text(y[r],m[r],col='red',labels='RT50',cex=1.2,pos=4)
    points(y[a], m[a], col='red')
    text(y[a],m[a],col='red',labels='RT10',cex=1.2,pos=4)

    #slope
    v <- 1
    b <- 1
    p <- array()

    while(b<NROW(m))
    {
      p[b] = (m[b+1]-m[b])/(y[b+1]-y[b])
      b = b+1
    }
    smax<-which.max(p)
    smin<-which.min(p)
    points(y[smax],m[smax],col='green')
    text(y[smax],m[smax],col='green',labels='maxSlope',cex=1.2,pos=4)
    points(y[smin],m[smin],col='green')
    text(y[smin],m[smin],col='green',labels='minSlope',cex=1.2,pos=4)

    r4=max(m)-m[1]   #F/F0

    #Tau
    n1<- tail(m, NROW(m)-e)
    n2<- which.min(abs(n1-(1/exp(1)*(max(n1)-min(n1))+min(n1))))
#exp(1) = e (Euler)
    n2=n2+e
    Tau <- y[n2]-y[e]
    points(y[n2],m[n2],col='purple')
    text(y[n2],m[n2],col='Purple',labels='Tau',cex=1.2,pos=4)

    min <- m[1]
    max <- max(m)
    Amplitude <- r4
    maxSlope <- max(p)
    minSlope <- min(p)
    RT50 <- y[r] - y[e]
    RT10 <- y[a] - y[e]
    TtP  <- y[e] - y[1]

    #save data
    title(main=name)
    mydata <- matrix(c(name,min,max,Amplitude,maxSlope,minSlope,Tau,RT50
,RT10,TtP),nrow=1,ncol=10)
    library(XLConnect)
    ExcelFile <- '/Users/chris/Desktop/mydatanew.xlsx'
    wb <- loadWorkbook(ExcelFile)
    appendWorksheet(wb, mydata, sheet = "Sheet1")
    saveWorkbook(wb,ExcelFile)
    return(mydata)
}
```

```
#Caffeine response analysis
Caffeine <- function() {

  filename <- file.choose()
  data <- read.csv(filename, header=T, sep='\t')
  name <- basename(filename)

  Transient <- data$Intensity.Region.1 - mean(data$Intensity.Region.2, n
a.rm=T)
  Time <- data$Time..s.

  #F/F0
  F0 <- min(Transient)
  Transient = Transient/F0

  #Filtering
  x <- filter(Transient, rep(1,16)/16)
  y <- Time
  sensitivity <- 0.99  # 0.97 for caff, inc to 0.99 if not every valley
is detected

  i = 61
  j = 1
  h = 0
  dummy = 2
  max = NROW(x)
  valleyarray <- array(1:10)
  timearray <- array(1:10)
  position <- array(1:10)

  plot(Time, x,type='l', xlab="Time[sec]", ylab="Intensity F/F0")
  timearray[1]=10

  #find valley
  while((max-61)>i) {
    if(x[i]<x[i-10] & x[i]<x[i+10] & x[i]<(sensitivity*x[i+45])){ #i+15

      if((y[i]-timearray[dummy-1]) < 0.1) {
        valleyarray[dummy-1] = x[i]
        timearray[dummy-1] = y[i]
        position[dummy-1] = i
      }
      else {
        valleyarray[dummy] = x[i]
        timearray[dummy] = y[i]
        position[dummy] = i
        dummy = dummy+1
        h=h+1
      }
      i = i+1
    }
    else {
      i = i+1
```

```
    }
  }

  while(j<dummy) {
    points(timearray[j],valleyarray[j])
    j=j+1
  }

  max1 <- which.max(x)
  min1 <- which.min(x)
  e3 <- peak(x,y)  # maxAmplitude before Caff

  Incr <- (x[max1]-x[min1])/(e3-x[min1])*100 #Inc in %


  points(y[max1],x[max1], col='blue')
  x[is.na(x)] <- 0
  x <- x[x!=0]

  # RT50, RT10

  e<- which.max(x)
  n<- tail(x, NROW(x)-e)  # only dec
  r<- which.min(abs(n-(0.5*(max(n)-valleyarray[j-1])+valleyarray[j-1])))
  a<- which.min(abs(n-(0.1*(max(n)-valleyarray[j-1])+valleyarray[j-1])))
  r=r+e # add points to max
  a=a+e

  points(y[r], x[r], col='red')
  text(y[r],x[r],col='red',labels='RT50',cex=0.6,pos=4)
  points(y[a], x[a], col='red')
  text(y[a],x[a],col='red',labels='RT10',cex=0.6,pos=4)
  RT50 = y[r]-y[e]
  RT10 = y[a]-y[e]

  #Tau
  n1<- tail(x, NROW(x)-e)
  n2<- which.min(abs(n1-(1/exp(1)*(max(n1)-valleyarray[j-1])+valleyarray
[j-1])))  #exp(1) = e (Euler)
  n2=n2+e
  Tau <- y[n2]-y[e]
  points(y[n2],x[n2],col='purple')
  text(y[n2],x[n2],col='Purple',labels='Tau=',cex=0.6,pos=4)
  text(y[n2+400],x[n2],col='Purple',labels=Tau,cex=0.6,pos=4)

  #slope
  v <- 1
  b <- 1
  p <- array()
  e1 <- which(y==timearray[j-1])

  while(b<(NROW(x)-e1))
  {
    p[b+e1] = (x[b+1+e1]-x[b+e1])/(y[b+1+e1]-y[b+e1])
```

```
    b = b+1
  }

  smax<-which.max(p)
  smin<-which.min(p)
  points(y[smax],x[smax],col='green')
  text(y[smax],x[smax],col='green',labels='maxSlope',cex=0.6,pos=1)
  points(y[smin],x[smin],col='green')
  text(y[smin],x[smin],col='green',labels='minSlope',cex=0.6,pos=4)

  title(main=name)

  maxSlope = p[smax]
  minSlope = p[smin]
  TtP = y[e]-timearray[j-1]
  Amplitude = x[e]-valleyarray[j-1]

  mydata <- matrix(c(name,Amplitude,Incr,maxSlope,minSlope,Tau,RT50,RT10
,TtP),nrow=1,ncol=9)

  #save data
  library(XLConnect)
  ExcelFile <- '/Users/chris/Desktop/mydataTest2.xlsx'
  wb <- loadWorkbook(ExcelFile)
  appendWorksheet(wb, mydata, sheet = "Sheet1")
  saveWorkbook(wb,ExcelFile)
  return()
}

#peak detection for Caffeine Response
peak <- function(x,y) {

  i = 60
  j = 1
  ka = 0
  dummy = 2
  max = NROW(x)
  peakarray <- array(1:10)
  timearray <- array(1:10)
  position <- array(1:10)

  sensitivity <- 1.04 #change according to loop (change in 0.01 steps; d
own for higher sens, start at 1.04)

  while((max-65)>i) {

    if(x[i]>x[i-10] & x[i]>x[i+10] & x[i]>(sensitivity*x[i+45])){
      ka=ka+1
      if((y[i]-timearray[dummy-1]) < 0.1) {
        peakarray[dummy-1] = x[i]
        timearray[dummy-1] = y[i]
        position[dummy-1] = i
      }
      else {
```

```
        peakarray[dummy] = x[i]
        timearray[dummy] = y[i]
        position[dummy] = i
        dummy = dummy+1
      }
      i = i+1
    }
    else {
      i = i+1
    }
  }

  while(j<dummy-1) {
    points(timearray[j+1],peakarray[j+1])
    j=j+1
  }
  return(peakarray[j-3]) #only -2 if last peak is not detected (j-1)
}
```

Statistics and Graphs

```
Statistics <- function() {

  library(readxl)
  library(plyr)s
  x<-read_excel("/Users/chris/Desktop/Experiments/ExcelData/WorkingWith_
plusNEW.xlsx", 'SorafenibNEW', col_names = T)
  Time <- x$Time
  Time[is.na(Time)] <- 0
  Amplitude <- x$Amplitude
  Amplitude[is.na(Amplitude)] <- 0
  Treatment <- x$Treatment
  Treatment[is.na(Treatment)] <- 0
  maxS <- NROW(x)
  Time <- strtoi(Time)

  #exclude ISO/NT/Time points>13
  g <- 1
  h <- 1
  excl<-array()
  while(maxS>=g) {
    if(Treatment[g]=='Iso'||Treatment[g]=='NT'||Time[g]>13) {
      excl[h] = g
      h=h+1
    }
    g=g+1
  }
  x <- x[-excl,]
  x$Time <- strtoi(x$Time)
  Time <- x$Time
  Amplitude <- x$Amplitude
```

```
  Treatment <- x$Treatment

  #graph
  gp <- data_summary(x, varname="Amplitude", groupnames=c("Treatment", "
Time"))

  par(mfrow=c(1,2))
  library(ggplot2)
  gp[is.na(gp)] <- 0
  gp$Time <- strtoi(gp$Time)
  gp <- gp[order(gp$Time),]
  gp$Treatment <- factor(gp$Treatment, levels=c("Sora","DMSO"), label=c(
"Sorafenib","Control"))

  g <- ggplot(gp, aes(x=Time-1, y=Amplitude, group = Treatment, shape=Tr
eatment, linetype=Treatment))+
    geom_errorbar(aes(ymin=Amplitude-sem, ymax=Amplitude+sem), width=.5,
                  position=position_dodge(0.0)) +
    geom_line(size=1.0) +
    geom_point(size=3.2)+
    labs(title="Amplitude",x="Time[min]", y = "Amplitude[msec]")+
    theme_classic()+
    scale_x_continuous(breaks = round(seq(min(gp$Time-1), max(gp$Time),
by = 2),1))+
    theme(legend.background = element_rect(colour = "black"))+
    theme(legend.title=element_blank())+
    theme(legend.key.size=unit(1.5,"cm"))+
    theme(legend.text=element_text(size=20))+
    theme(legend.position=c(0.2,0.8))+
    theme(text = element_text(size=30))+
    scale_linetype_manual(values=c("solid", "dotted"))

  print(g)
  print(gp)
  ggsave('Amplitude.pdf', path='/Users/chris/Desktop/Thesis/PicsOverT',
width = 30, height = 20, units = 'cm', dpi=600)
  #end graph

  #mixed anova
  library(stats)

  #Convert variables to factorials
  x <- within(x, {
    Treatment <- factor(Treatment)
    Time <- factor(Time)
    Cell <- factor(Cell)
  })

  library(nlme)
  library(lme4)
  model<-lme(Amplitude~Treatment*Time,random=(~1|Cell/Time), data=x)
  model <- anova(model)
  print(model)
```

```
  #post-hoc
  t <- pairwise.t.test(x$Amplitude, x$Treatment, p.adj = 'fdr', paired=T
)
  print(t)

  dataSora <- subset(x, Treatment == 'Sora')
  dataControl <- subset(x, Treatment == 'DMSO')

  v <- 1
  u <- array()
  while(v<14) {
   dataSoraB <- subset(dataSora, Time==v)
   dataControlB <- subset(dataControl, Time==v)

   u <- t.test(dataSoraB$Amplitude, dataControlB$Amplitude)
   print(list(v,u))
   v=v+2
  }

  aC <- pairwise.t.test(dataControl$Amplitude, dataControl$Time, p.adj =
"bonf")
  aS <- pairwise.t.test(dataSora$Amplitude, dataSora$Time, p.adj = "bonf
")

  print(list(aC,aS))

  print(summary(aC))
  return(summary(aS))

  #end post hoc
}


data_summary <- function(data, varname, groupnames){
  require(plyr)
  summary_func <- function(x, col){
    c(mean = mean(x[[col]], na.rm=TRUE),
      sem = (sd(x[[col]], na.rm=TRUE))/sqrt(length(x[[col]])))
  }
  data_sum<-ddply(data, groupnames, .fun=summary_func,
                  varname)
  data_sum <- rename(data_sum, c("mean" = varname))

  return(data_sum)
}
```

Statistics and Graphs (Isoproterenol)

```
Statistics <- function() {

  library(readxl)
  library(plyr)
  x<-read_excel("/Users/chris/Desktop/Experiments/ExcelData/WorkingWith_
plusNEW.xlsx", 'IsoproterenolNEWadaptedTime', col_names = T)
  Time <- x$Time
  Time[is.na(Time)] <- 0
  Amplitude <- x$Amplitude
  Amplitude[is.na(Amplitude)] <- 0
  PreIsoTreatment <- x$PreIsoTreatment
  PreIsoTreatment[is.na(PreIsoTreatment)] <- 0
  maxS <- NROW(x)
  Time <- strtoi(Time)


  #exclude NT/Time points>5
  g <- 1
  h <- 1
  excl<-array()
  while(maxS>=g) {
    if(PreIsoTreatment[g]=='x'||Time[g]>5) {
      excl[h] = g
      h=h+1
    }
    g=g+1
  }
  x <- x[-excl,]
  x$Time <- strtoi(x$Time)
  Time <- x$Time
  Amplitude <- x$Amplitude
  PreIsoTreatment <- x$PreIsoTreatment

  #graph
  gp <- data_summary(x, varname="Amplitude", groupnames=c("PreIsoTreatme
nt", "Time"))

  par(mfrow=c(1,2))
  library(ggplot2)
  gp[is.na(gp)] <- 0
  gp$Time <- strtoi(gp$Time)
  gp <- gp[order(gp$Time),]
  gp$PreIsoTreatment <- factor(gp$PreIsoTreatment, levels=c("Sora","DMSO
"), label=c("Sorafenib","Control"))

  g <- ggplot(gp, aes(x=Time-1, y=Amplitude, group = PreIsoTreatment, sh
ape=PreIsoTreatment, linetype=PreIsoTreatment))+
    geom_errorbar(aes(ymin=Amplitude-sem, ymax=Amplitude+sem), width=.5,
                  position=position_dodge(0.00)) +
    geom_line(size=1.0) +
```

```
    geom_point(size=3.2)+
    labs(title="Amplitude",x="Time[min]", y = "Amplitude[msec]")+
    theme_classic()+
    scale_x_continuous(breaks = round(seq(min(gp$Time-1), max(gp$Time),
by = 2),1))+
    theme(legend.background = element_rect(colour = "black"))+
    theme(legend.title=element_blank())+
    theme(legend.key.size=unit(1.5,"cm"))+
    theme(legend.text=element_text(size=14))+
    theme(legend.position=c(0.7,0.45))+
    theme(text = element_text(size=16))+
    scale_linetype_manual(values=c("solid", "dotted"))

  print(g)
  print(gp)
  ggsave('IsoAmplitude.pdf', path='/Users/chris/Desktop/Thesis/PicsOverT
/Iso', width = 30, height = 20, units = 'cm', dpi=600)

  library(stats)

  # Convert variables to factorials
  x <- within(x, {
    PreIsoTreatment <- factor(PreIsoTreatment)
    Time <- factor(Time)
    Cell <- factor(Cell)
  })

  library(nlme)
  library(lme4)
  model<-lme(Amplitude~PreIsoTreatment*Time,random=(~1|Cell/Time), data=
x)
  model <- anova(model)
  print(model)
  t <- pairwise.t.test(x$Amplitude, x$PreIsoTreatment, p.adj = 'fdr', pa
ired=T)
  print(t)

  dataSora <- subset(x, PreIsoTreatment == 'Sora')
  dataControl <- subset(x, PreIsoTreatment == 'DMSO')

  v <- 1
  u <- array()
  while(v<7) {
    dataSoraB <- subset(dataSora, Time==v)
    dataControlB <- subset(dataControl, Time==v)

    u <- t.test(dataSoraB$Amplitude, dataControlB$Amplitude)
    print(list(v,u))
    v=v+2
  }

  return()

  aS <- aov(Amplitude ~ Time, dataSora)
```

```
  aC <- aov(Amplitude ~ Time, dataControl)

  aC <- pairwise.t.test(dataControl$Amplitude, dataControl$Time, p.adj =
"bonf")
  aS <- pairwise.t.test(dataSora$Amplitude, dataSora$Time, p.adj = "bonf
")

  print(summary(aC))
  return(summary(aS))

}


data_summary <- function(data, varname, groupnames){
  require(plyr)
  summary_func <- function(x, col){
    c(mean = mean(x[[col]], na.rm=TRUE),
      sem = (sd(x[[col]], na.rm=TRUE))/sqrt(length(x[[col]])))
  }
  data_sum<-ddply(data, groupnames, .fun=summary_func,
                  varname)
  data_sum <- rename(data_sum, c("mean" = varname))

  return(data_sum)
}
```

Western Blot Analysis and Bar Charts

```
Statistics <- function() {

  library(readxl)
  library(plyr)
  x<-read_excel("/Users/chris/Desktop/WB_Analysis/17:9:16/WB_Data 6,11,1
2,13,14,15.xlsx", 'R_PLB(meanCtrl)', col_names = T)

  SI <- subset(x, Treatment == 'S+I')
  DI <- subset(x, Treatment == 'D+I')
  D <- subset(x, Treatment == 'D')

  #Statistics

   #Check for power (change parameters accordingly)
  library(pwr)
  p <- pwr.anova.test(k=3,f=0.566,sig.level=.05,power=.8)
  print(p)

   #Check for homogeneity
  p <- bartlett.test(x$Ser16, x$Treatment)
  print(p)
```

```
   #Check for normality
  print(with(x, tapply(Ser16, Treatment, shapiro.test)))

   #non-parametric test
  x$Treatment <- as.factor(x$Treatment)
  p <- kruskal.test(x$Ser16 ~ x$Treatment)
  print(p)

  a <- anova(lm(Ser16 ~ Treatment, x))
  t <- pairwise.t.test(x$Ser16, x$Treatment, p.adj = 'fdr', paired=T)

  print(t)

  #Plot
  library(ggplot2)

  wb <- x$Ser16

  a <- aggregate(wb~Treatment, x, mean ) # calculate mean
  sd <- aggregate(wb~Treatment, x, sd )  # calculate sd
  sem = sd$wb/sqrt(length(wb)/3)         # calculate sem
  limits <- aes(ymax = a$wb + sem, ymin= a$wb)

  colour <- c("white","grey","black")    # set colour

   p <- ggplot(a, aes(factor(Treatment), wb))+
       theme_classic()+
       theme(axis.ticks.x=element_blank())+
       theme(axis.line=element_line(size=2))+

       labs(title="PLB_phSer16")+ #, x="Group",y="totalPLB")+
       xlab("")+ylab("")+
       theme(text = element_text(size=32, face="bold"))+
       geom_bar(stat="identity", fill=colour, width=0.4, colour="black",
size=1.8)+
       geom_errorbar(limits, width=0.2, size=1.4)+
       scale_x_discrete(labels=NULL)+ #labels=NULL
       scale_y_continuous(expand = c(0, 0), limits=c(0,50))    #change a
ccordingly

  ggsave('PLB_Ser16.pdf', path='/Users/chris/Desktop', width = 30, heigh
t = 20, units = 'cm', dpi=600)
  print(p)
  return()
}


data_summary <- function(data, varname, groupnames){
  require(plyr)
  summary_func <- function(x, col){
    c(mean = mean(x[[col]], na.rm=TRUE),
      sem = (sd(x[[col]], na.rm=TRUE))/sqrt(length(x[[col]])))
  }
```

```
  data_sum<-ddply(data, groupnames, .fun=summary_func,
                  varname)
  data_sum <- rename(data_sum, c("mean" = varname))

  return(data_sum)
}
```

Drugs used

Drug	Company	Catalog#	Lot#
2,3 Butanedione monoxime	Sigma	B0753	011M0033V
Bovine calf serum	Sigma	12133C	12133C
Caffeine	Sigma	C0750	021M0092V
Calcium chloride solution (1M in H_2O)	Sigma	21115	*
Cell Lysis Buffer (10x)	Cell Signaling	9803S	*
Clarity™ Western ECL Blotting Substrates	Bio-Rad	10026384	*
D(+) Glucose	Merck	108337	K44709637347
Dimethyl sulfoxide	Sigma	D5879	SHBG7041V
Forane® (Isofluran)	AbbVie	B506	*
Fluo-4/AM	Thermo Fisher	F14201	1726528
Heparin 5000I.E./ml	Gilvasan	3909981	3L646A
HEPES	Sigma	H3375	SLBH9885V
Isoproterenol hydrochloride	Sigma	I5627	037K1231
Laminin (1mg/ml)	Sigma	L2020	105M4075V
Liberase TM Research Grade	Roche	05401127001	10829800
Magnesium chloride hexahydrate	Merck	105833	A0344733414
Magnesium sulfate heptahydrate	Merck	105886	A892986734
2-Mercaptoethanol	Bio-Rad	1610710	*
Methanol	Merck	106009	I801009542
Milk (powdered)	Roth	T1452	146238370
Pluronic F-127	Thermo Fisher	P3000MP	*
Ponceau S solution	Sigma	P7170	SLBD310LV
Potassium chloride	Sigma	P5405	SLBH5524V
Potassium phosphate monobasic	Sigma	P9791	110M0202V
Precision Plus Protein™ All Blue Prestained Protein Standards	Bio-Rad	1610373	*
Phenylmethanesulfonyl fluoride	Sigma	P7626	*
Sodium chloride	Sigma	71380	SZBF0300V
Sodium phosphate dibasic heptahydrate	Sigma	S9390	108K0169
Sorafenib (Bay 43-9006)	Bio Vision	159425	*
Spectra™ Multicolor Low Range Protein Ladder	Thermo Fisher	26628	*
Stripping buffer (Restore™ PLUS Western Blot)	Thermo Fisher	46430	RE233374
SuperSignal™ West Femto Maximum Sensitivity Substrate	Thermo Fisher	34096	*
SuperSignal™ West Pico Maximum Sensitivity Substrate	Thermo Fisher	34080	*
Taurine	Sigma	T0625	BCBJ5897V
Tricine Sample Buffer	Bio-Rad	1610739	350002895

Drug	Company	Catalog#	Lot#
Trypsin 2.5% (10x)	Thermo Fisher	15090	1581628
TTS Buffer (10x)	Bio-Rad	1610744	1320892
XT MOPS Running Buffer (20x)	Bio-Rad	1610788	*
XT Reducing Agent (20x)	Bio-Rad	1610792	*
XT Sample Buffer (4x)	Bio-Rad	1610791	*

* More than one Lot# used / Lot# could not be obtained

Antibodies used

Antibody	Company	Catalog#	Lot#
Anti-Mouse IgG	GE Healthcare	NA931V	7141636
Anti-Rabbit IgG	GE Healthcare	NA934V	9720457
GAPDH	Cell signaling	D16H11	6
PLB total	Badrilla	A01014	642026
PLB phSer16	Badrilla	A01012	64202
PLB phThr17	Badrilla	A01013AP	140901
CaMKII total	Cell signaling	D11A10	3
CaMKII phThr286	Abcam	ab32678	GR1089471